University of Bahrain

Department of Physics

PHYCS425: Computational Physics

Fall 2021

Constrained motion on surfaces

Instructor

Dr. Jawad Mohamed Taher Mohamed Alsaei

Authors

Ali Mirza Isa	20186917
Asif Bin Ayub	20191251
Kumail Abdulaziz Radhi	20196080

Contents

1 Introduction

Imagine you're on a roller coaster. You're plunging downwards from a ramp at dizzying speeds. You're terrified, but not afraid for your life*. You know that no matter what happens, you'll always remain on the track. This is an example of constrained motion, and it is virtually everywhere. An athlete skiing down an icy mountain, a car driving down a road† are instances of constrained motion on surfaces.

There are other forms of constrained motion, like that of a fluid moving in a pipe. But our focus in this project is only on the former. These types of constraints fall under the category of "holonomic constraints". For each one of these constraints, the system loses a degree of freedom.

If one wants to investigate such motion analytically, Newton's laws of motion are not really helpful. One usually resorts to Lagrangian or Hamiltonian mechanics to get any sort of insight from these systems. Even then, getting exact solutions is cumbersome, and when damping is added, it becomes exponentially more difficult to obtain. This is where computer simulations come in handy. They allow us to study the properties of motion without knowing the most general form of the solution.

In this project, we will explore constrained motion on various surfaces in both 1D & 2D. In part I, we'll investigate the motion on 2 curves: a parabola (C_1), and an unknown curve (C_2), which we have to identify. We also find the equilibrium points for both. We study the periodic motion in detail, exploring the effect of various parameters like the dimension of the curves & initial displacement. We then add damping and driving forces to the systems and investigate the possibility of chaotic motion.

In part II, we have a spherical surface. We investigate the initial conditions that lead various paths – including closed paths and Lissajous-like figures. Here too, we investigate if chaotic motion is possible. In addition, we study the effects of a homogeneous damping force. And then we study the motion on a hemispherical surface.

In all cases, we used 4^{th} order RK4 method to integrate our equations of motion. The conservation of energy and angular momentum were checked wherever relevant.

Buckle up, because you don't want to fall off this roller coaster!

* Assuming the roller coaster was well maintained
† Unless the car is in a rally race

2 Theory

2.1 The Runge-Kutta method[1]

Since we used 4th order Runge-Kutta method (or RK4) throughout this project, it is worthwhile to go over some aspects of this method. But first, some historical context. Back in 1895, Carl Runge thought he could outsmart Euler by coming up with a numerical method more accurate than Euler. Euler's method was to approximate solutions to initial value problems by dividing the motion into finite intervals and assuming the slopes stay constant between intervals. The slope at each point determines the next point.

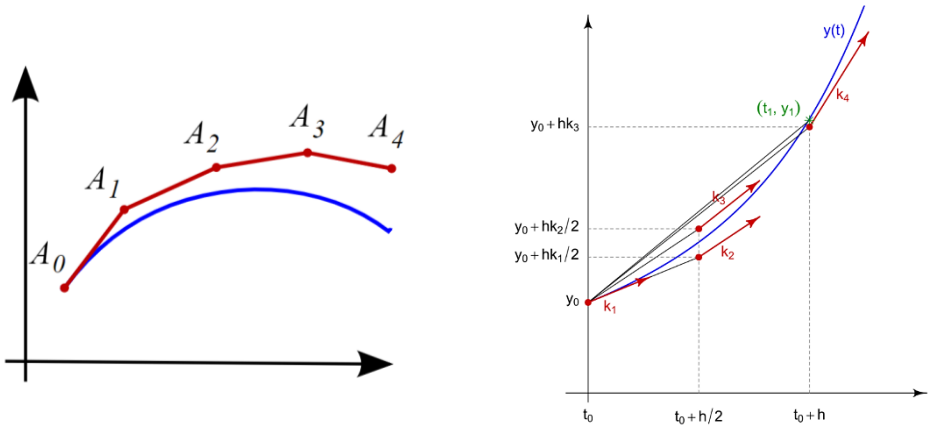

Illustration of Euler method (left) & RK4 (right) [Source: Wikimedia Commons]

RK4 method improves upon Euler by taking a combination of 4 weighted slopes instead of just one (illustrated in the figure above). The result is a much improved local truncation error (error accumulated in one step of size h) of $O(h^5)$ compared to Euler method's $O(h^2)$. And the total accumulated error also sees an improvement: with RK4's $O(h^4)$ compared to Euler's $O(h)$.

And unlike Euler method, RK4 has a time-symmetric definition, meaning it can better represent physical systems, which have this property.

2.2 Holonomic systems[2]

As we stated in the introduction, we deal in this project with holonomic constraints, where the position and time coordinates of a system are related to each other by a function of the form:

$$f(x_1, x_2, x_3, \dots x_n, t) = 0$$

Here, $x_1, x_2, \dots, x_n$ are the position coordinates in an n-dimensional space.

A holonomic system is one in which all of the constraints are holonomic. To give a concrete example, a simple pendulum is a holonomic system. In simple pendulum, a mass is attached to a string of fixed length ℓ, and the path of the pendulum is along a circle of length ℓ at all times, i.e. $(x - x_0)^2 + (y - y_0)^2 = \ell^2$ for a pendulum pivoted at (x_0, y_0). Another example is the motion of a rigid body.

Holonomic constraints reduce the degrees of freedom of the system. In our project we see in part I that despite the curves being in a 2D space, we only require one piece of information, θ, to track the particle throughout its motion. Similarly, in part II, despite being embedded in a 3D space, we only need to track θ & φ to determine the position of the particle.

2.3 Chaotic motion

Edward Lorenz, one of the pioneers in the field of chaos defined it as follows: "*Chaos: When the present determines the future, but the approximate present does not approximately determine the future.*"

This sums up chaotic behaviour very nicely. Chaotic motion doesn't mean that we can't predict what will happen to a system given certain initial conditions. It means that if we start from different initial conditions that are close give rise to disparate behaviour as time progresses. This sensitivity to initial conditions is one of the key markers of chaos. Another sign that a system is chaotic is loss of periodicity.

Chaotic systems occur in a diversity of situations. From predator-prey populations to financial models, weather patterns to the rhythms of heartbeat, chaos is always hiding around the corner. But not all chaotic systems are equal. The route a system follows leading to chaos is not unique.[3] The most familiar one is the period-doubling route. Other routes include: the intermittency route, Ruelle-Takens-Newhouse route and the crisis route.

A definitive test to detect chaotic motion and the route to chaos is to calculate the **Lyapunov exponent**.[4] It measures the sensitivity of a system to initial conditions. Depending on the magnitude and sign of this parameter, one can find out if a given system is chaotic.

3 Part I: Constrained motion in 1D

3.1 Oscillatory motion & equilibrium points

Trying out different initial conditions, we could confirm that a particle undergoes oscillatory motion on both curves C_1 & C_2. This corresponds to closed paths in the phase space. Shown below are the phase space portraits corresponding to the different initial conditions for both curves. The time-step dt was $0.01s$ throughout this project.

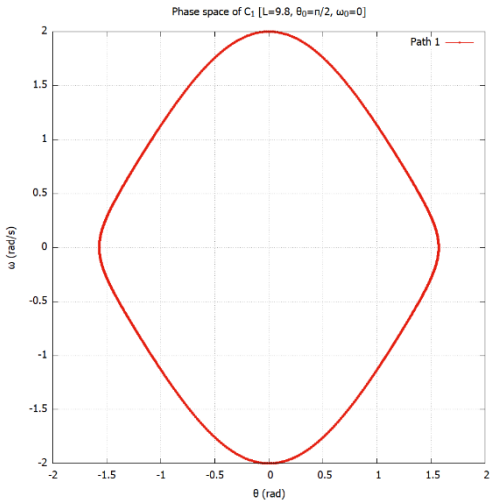

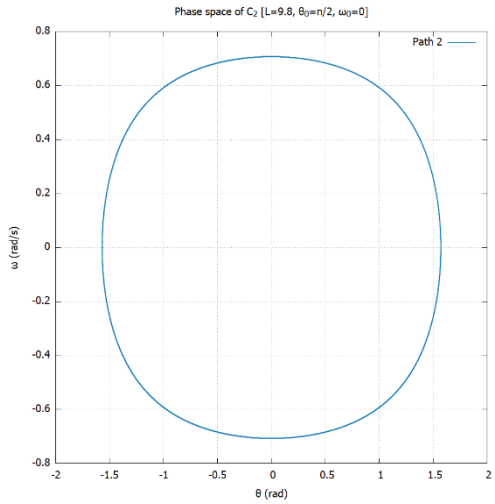

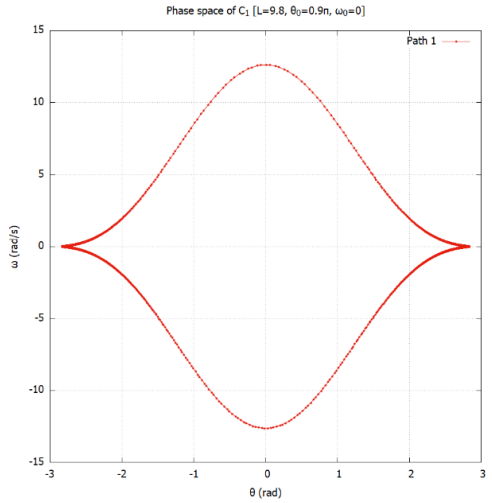

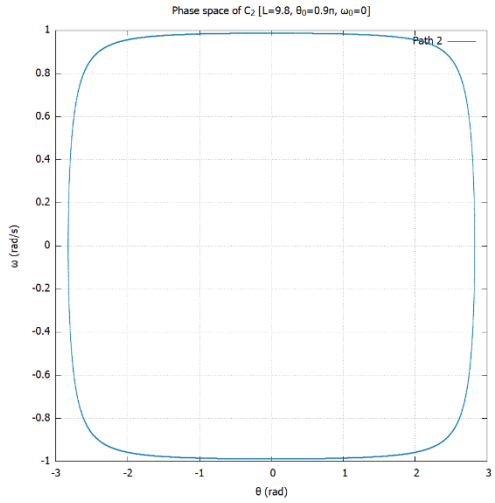

Closed paths in the phase space correspond to oscillatory motion. For C_1, this is replicated for all initial conditions in the allowed range $-\pi < \theta_0 < \pi$.*

* Unless mentioned otherwise, angles are in rad, angular velocities are in rad/s, time is in seconds

For C_2, if the initial velocity exceeds a certain limit, the motion is no longer constrained, and the object escapes the curve entirely and it is not oscillatory.

Classically, equilibrium points correspond to the points where the potential energy of the system is either a local minima or maxima. This corresponds to the points where the net force/torque acting on an object is 0. For determining equilibrium points, we checked at what instances of motion the angular acceleration ($\ddot{\theta}$ or `der_omega` in the code) is close to 0, up to some tolerance.

We found that both curves have one equilibrium point each, corresponding to $\theta \approx 0$. For the parabola (C_1), this corresponds to its vertex, the point at which the gravitational potential is minimum. And as we will find out later on in this report, the equilibrium point for C_2 is also where gravitational potential is minimum.

Knowing that the potential energy at equilibrium points is minimum, we can conclude that these points are points of *stable equilibrium*. This will be further justified when we look at the phase portraits of damped motion.

3.2 Dependence of oscillation period (T) on the oscillation amplitude (θ_0)

For C_1, we find that the period increases steadily as the oscillation amplitude increases. Remarkably, for C_2, the period remains constant as we change the oscillation amplitude. This is an important clue that will be used to identify C_2 later on. The graph below shows the change in period when $\ell = g = 9.8\ m$

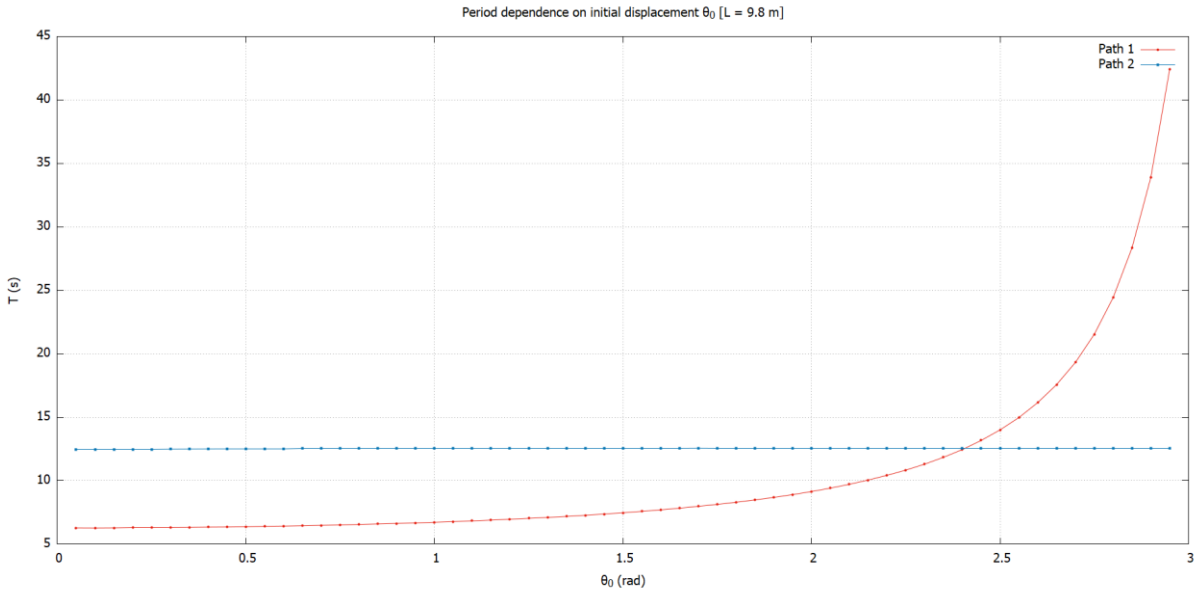

To get this graph, we had to figure out a way to measure the period from the code. We summarise our method below.

Firstly, we note that C_1 is symmetric about $\theta = 0$. This is also evidenced in the phase portraits above. We can therefore study the effect of amplitude between $0 \leq \theta_0 < \pi$. The behaviour of period will be mimicked in $-\pi < \theta \leq 0$. This symmetry also applies to C_2, so we can use this for C_2 as well.

To simplify the period measurement, we choose the initial angular velocity ω_0 to be 0. This means that the initial displacement θ_0 corresponds to the oscillation amplitude. To measure the period (T), we checked when the system returned to its initial conditions (θ_0, ω_0). This meant checking when angular velocity $\omega(t)$ came close to 0 ($\because \omega_0 = 0$), up to some tolerance and $\theta_0 > 0$.

Fitting the T vs θ_0 graph for $\ell = g = 9.8$ m:

- For C_2, the relation is quite straightforward. The period is constant around 4π. So, we may write:

$$T_2(\ell = g) = 4\pi$$

- For C_1, the relation is much less obvious. For all we know, there may not even be a closed form expression for the period. After fiddling around randomly with various functions, we struck (fool's) gold. When we try to fit the graph above with the equation below, we get a really good fit (~3.36% error).

$$T_1 \approx \frac{2\pi}{\sqrt{1 - \sin^4 \frac{\theta_0}{2}}}$$

3.3 Dependence of oscillation period (T) on the length parameter (ℓ)

We repeat the same analysis as above for this part. Except here, we loop over different length parameters ℓ instead of oscillation amplitude. The period measurement is done in e exact same way. This is the graph we obtained for $\theta_0 = \frac{\pi}{2}, \omega_0 = 0$.

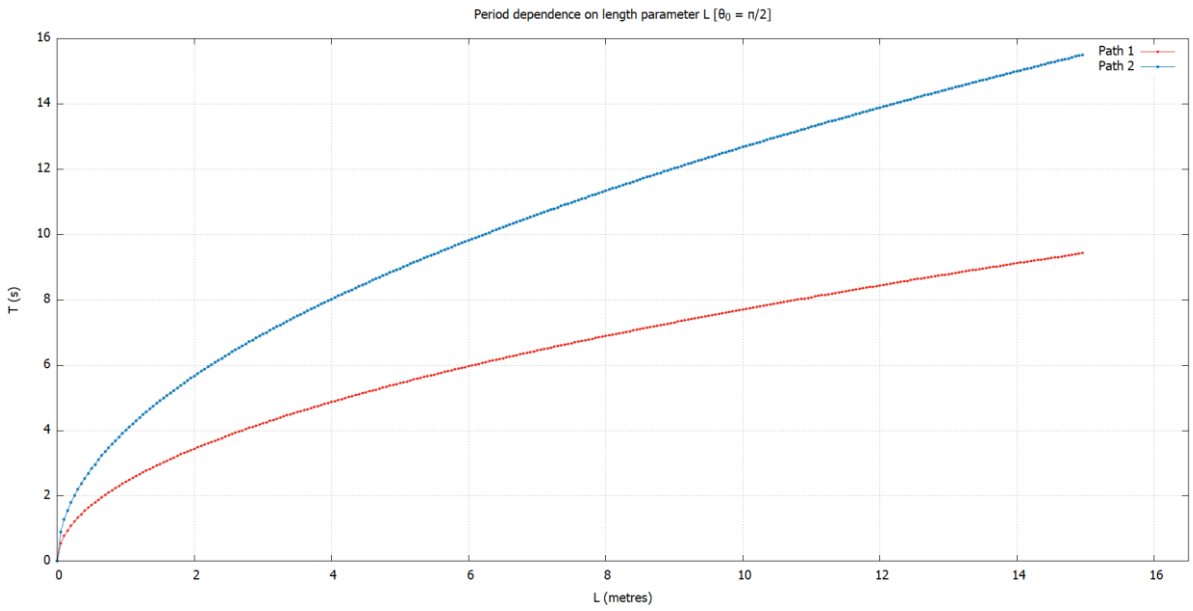

The results here are a bit more similar. The period increases as we increase ℓ. Physically, this makes sense, as making the curve bigger means a longer distance to travel, increasing the period. We find that for both C_1 & C_2, the period is proportional to the square root of ℓ. This was verified by fitting the data using expressions of the form $f = \sqrt{ax + b}$ in Gnuplot.

$$\text{i. e. } T_1 \propto \sqrt{\ell}, \qquad T_2 \propto \sqrt{\ell}$$

3.4 (Optional) General expression for period (T) as a function of θ_0, ℓ

- **Curve C_2:**

  The equation for curve C_2 is quite straight forward. From section 3.3, we saw that $T_2 \propto \sqrt{\ell}$. With a bit of dimensional analysis, we can figure out that for the units to match on both sides, we must somehow get rid of length units and add some time units to the LHS. There is really only one parameter in our system that can do this job, and that is the acceleration due to gravity (g) which has units of m/s^2.

  We can show that: $T_2 \propto \sqrt{\frac{\ell}{g}}$

  But, from section 3.2, we know that when $\ell = g$, $T_2 = 4\pi$. So, we may write:

$$\boldsymbol{T_2 = 4\pi\sqrt{\frac{\ell}{g}}}$$

  With some testing, this turns out to be a really accurate expression. We suspect that this expression can be derived analytically as well, but we'll leave that to others.

- **Curve C_1:**

  Taking inspiration from our analysis for C_1, we may deduce a similar expression for the period of curve C_1. We propose the following formula:

$$\boldsymbol{T_1 \approx \frac{2\pi\sqrt{\ell/g}}{\sqrt{1 - \sin^4\frac{\theta_0}{2}}}}$$

  While this is by no means a great approximation, it is better than having to stab at the dark. But if someone's life depends on the accurate prediction of period of an object moving along a parabolic ramp, don't count on this formula.

Notice how both expressions above are symmetric with respect to θ_0. Also note how the period of curve C_2 is exactly twice that of a simple pendulum for small angles. The period of C_1 diverges to infinity at $\theta_0 = \pm\pi$. This makes sense, as this corresponds to the end-points of the parabola, which are at infinite distance.

3.5 Identifying the curve C_2

We saw back in section 3.2 that the period of curve C_2 is independent of the oscillation amplitude θ_0. This was not some run-of-the-mill coincidence. This is a property of very special curves known collectively as "Tautochrones". For these curves, no matter where an object starts out along the curve, the time taken to reach the bottom is the same. The most famous of which is the cycloid. (Apparently there are infinitely many tautochrones)*

Naturally, we had to try the cycloid. But which one do we try? The traditional cycloid with parametric equation $\ell(\theta - \sin\theta\,, 1 - \cos\theta)$ looks like this when we take $-\pi < \theta < \pi$:

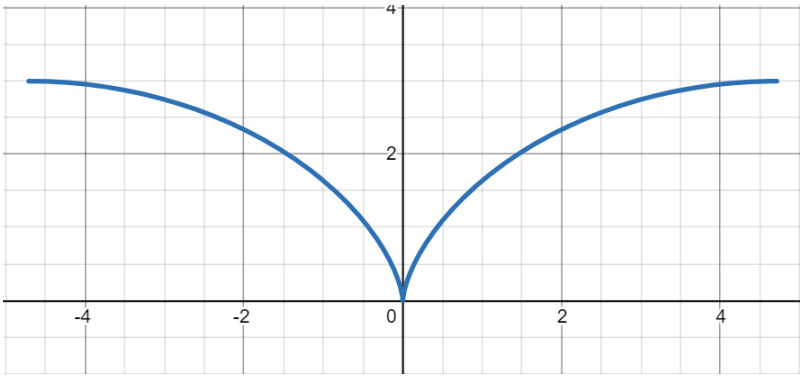

Intuitively, this does not look like a surface that can have constrained motion (due to its convexity). A more plausible cycloid may be the one with the equation $\ell(\theta + \sin\theta\,, 1 - \cos\theta)$, which looks like this for $-\pi < \theta < \pi$:

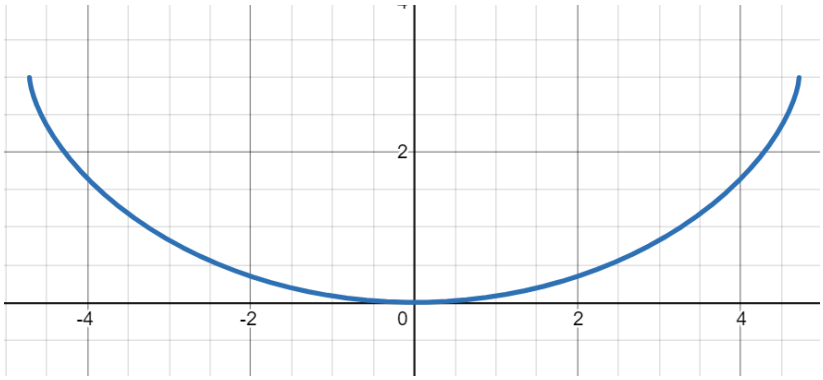

Now, how do we know if this is in fact the curve that we have at hand? There is only one way to find out, and that is to derive the equation of motion and see if it results in the same one given to us.

This means writing the Lagrangian of the system and obtaining the Euler-Lagrange equations for all degrees of freedom. A brief derivation is given below:

* See: Is the tautochrone curve unique?: American Journal of Physics: Vol 84, No 12 (scitation.org)

$$\mathcal{L} = T - V = \frac{1}{2}mv^2 - mgz = \frac{m}{2}[\dot{x}^2 + \dot{z}^2] - mgz$$

$$\text{or,} \qquad \mathcal{L} = \frac{m\ell^2}{2}\left[1 + \cos\theta\,\dot{\theta} + \dot{\theta}^2\right] - mg\ell[1 - \cos\theta]$$

The corresponding Euler-Lagrange equation is given by (only one degree of freedom):

$$\frac{\partial \mathcal{L}}{\partial \theta} = \frac{d}{dt}\left\{\frac{\partial \mathcal{L}}{\partial \dot{\theta}}\right\} \Rightarrow \ddot{\theta} = \frac{\sin\theta\left[\dot{\theta}^2 - \frac{g}{\ell}\right]}{2[1 + \cos\theta]}$$

This is exactly identical to the equation of motion we were given, so we have our C_2, namely: $\boldsymbol{\ell(\theta + \sin\theta\,, 1 - \cos\theta), -\pi < \theta < \pi}$

Note that translating the cardioid along z by a constant doesn't change the equation of motion. So, the cardioid in question is not unique.

While we're discussing the shape of the curves, let's see what C_1 looks like. For C_1, the origin coincides with the focus of the parabola. And as we've stated before, the equilibrium point ($\theta = 0$) is the lowest point of the curve in each case. This corresponds to the point $\left(0, -\frac{\ell}{2}\right)$ for C_1 and (0,0) for C_2.

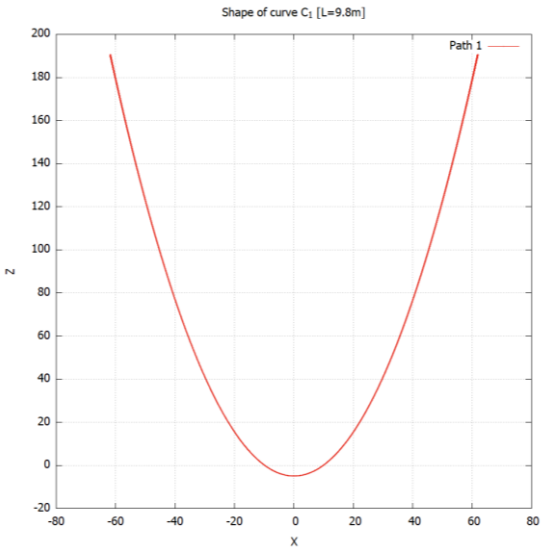

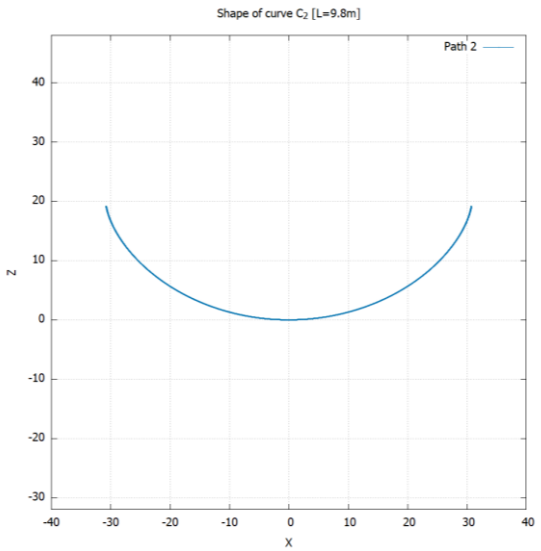

3.6 Adding damping and driving forces, chaos (?)

Firstly, how does one achieve a damping force for particles moving on curves practically? The solution we came up with is to imagine the entirety of the curve immersed in a viscous fluid. We assumed that the drag force is a linear one, proportional to the angular speed $\dot{\theta}$, but acting opposite to it. The strength of the drag force changes depending on the drag coefficient q (with unit s^{-1}). So, our equations of motion are now:

$$\ddot{\theta} = -\frac{g}{2\ell}\sin\theta\,[1+\cos\theta] - \frac{3\dot{\theta}^2\sin\theta}{2(1+\cos\theta)} - q\dot{\theta} \quad \text{for } C_1$$

$$\ddot{\theta} = \frac{\sin\theta\left[\dot{\theta}^2 - \frac{g}{\ell}\right]}{2[1+\cos\theta]} - q\dot{\theta} \quad \text{for } C_2$$

Like all damped systems, the systems exhibit 3 distinct behaviours: underdamped, overdamped and critically damped motion. The figures below showcase the various possibilities.*

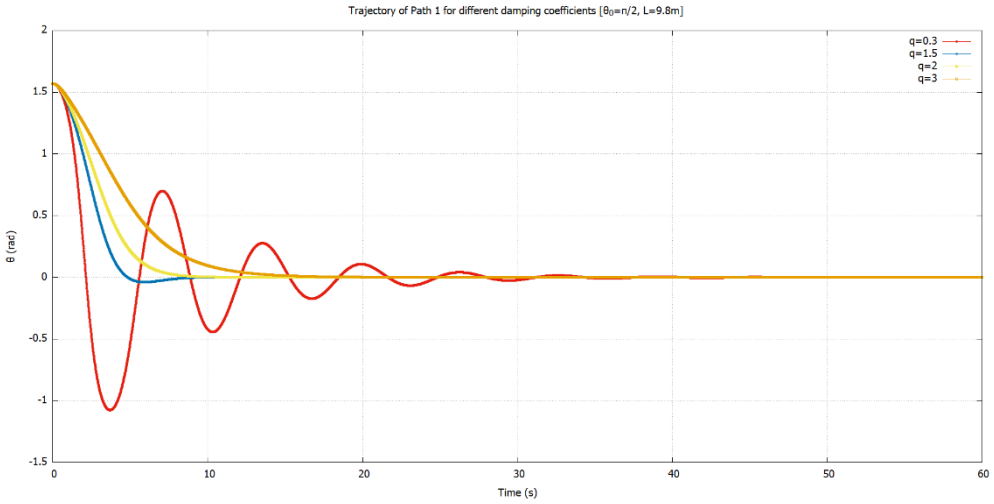

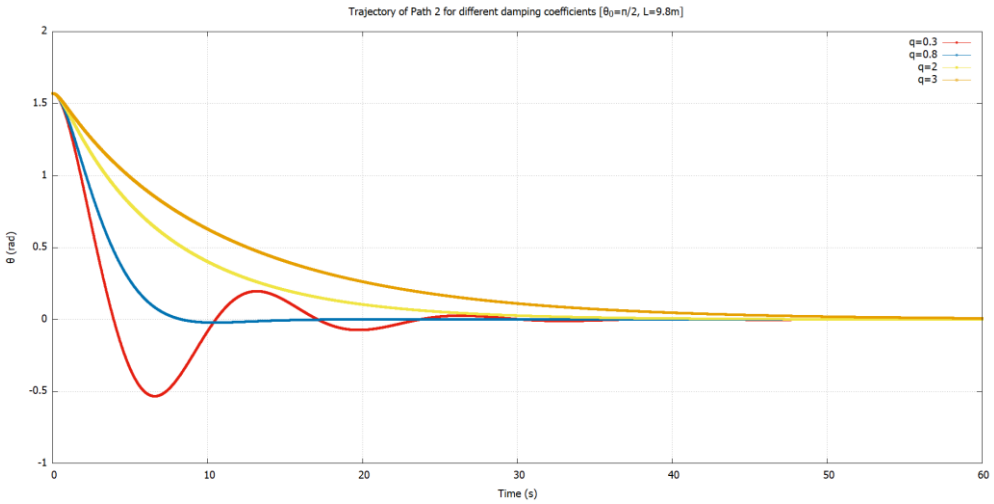

* The values of critical damping coefficients are not exact

As for adding a driving force, we just acquire an additional $F_D \sin \omega_D t$ term for both equations of motion (F_D has units of s^{-2}). That is:

$$\ddot{\theta} = -\frac{g}{2\ell}\sin\theta\,[1+\cos\theta] - \frac{3\dot{\theta}^2 \sin\theta}{2(1+\cos\theta)} - q\dot{\theta} + F_D \sin\omega_D t \qquad \text{for } C_1$$

$$\ddot{\theta} = \frac{\sin\theta\left[\dot{\theta}^2 - \frac{g}{\ell}\right]}{2[1+\cos\theta]} - q\dot{\theta} + F_D \sin\omega_D t \qquad \text{for } C_2$$

Usually, the effect of adding a sinusoidal driving force is as follows:

- For a fixed driving amplitude F_D, increasing the driving frequency ω_D decreases the oscillation amplitude. This is because the same energy is shared between more oscillations, meaning less energy per oscillation.
- For a fixed driving frequency ω_D, increasing the driving amplitude F_D increases the oscillation amplitude. Now, the system receives increasingly more energy.

So far, so good. Let us plot the oscillation amplitude for different ω_D, F_D and see if the above holds*. Below we have the variation of oscillation amplitude with ω_D.

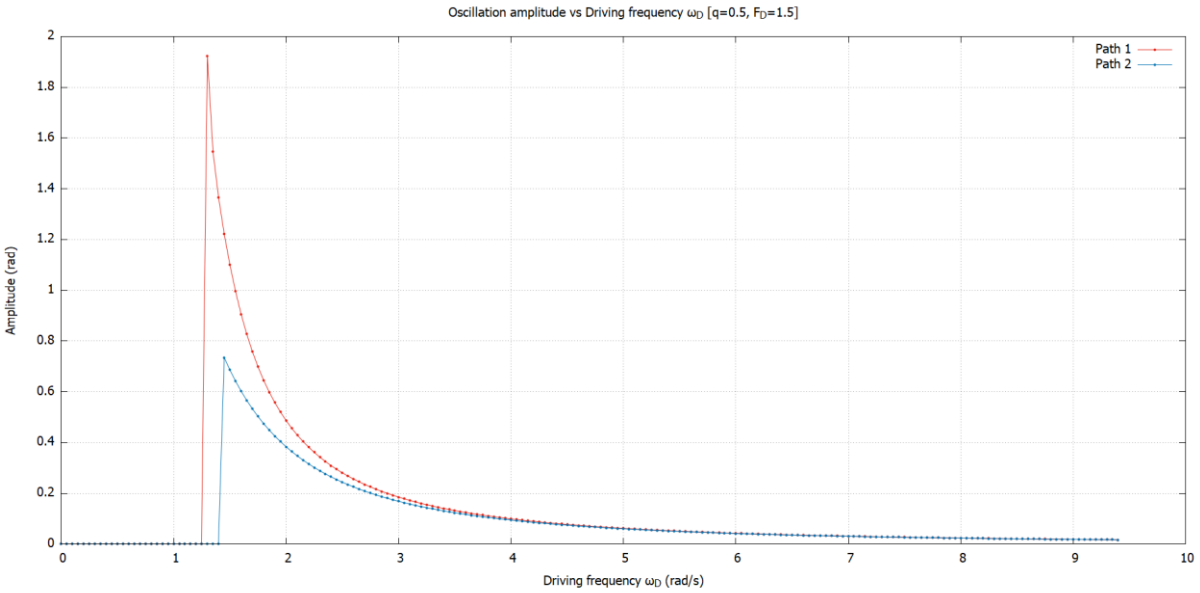

Hold on a second, I hear you ask. Why is the oscillation amplitude 0 for low frequencies? The answer is that it is not. In fact, there are no oscillations at all. When ω_D is low, the system never escapes the transient phase. θ shoots up to $\pm\infty$, indicating that the motion is no longer constrained. This is something that we encountered in section 3.1 for C_2.

* In all the amplitude plots, the amplitude was measured after a set time to account for the transient.

It makes sense that giving too much energy will cause the particle to escape for C_2. After all, it is a curve of finite length. But why it happens for C_1 is beyond us. A parabola is a curve of infinite length. And so the particle must always stay bound to the surface, no matter what energy is given to it. Perhaps it is the inaccuracies of simulation that is to blame. In all cases, we simulated the trajectory to verify this behaviour.

Shown below are plots for oscillation amplitude vs ω_D for several other driving amplitudes F_D.

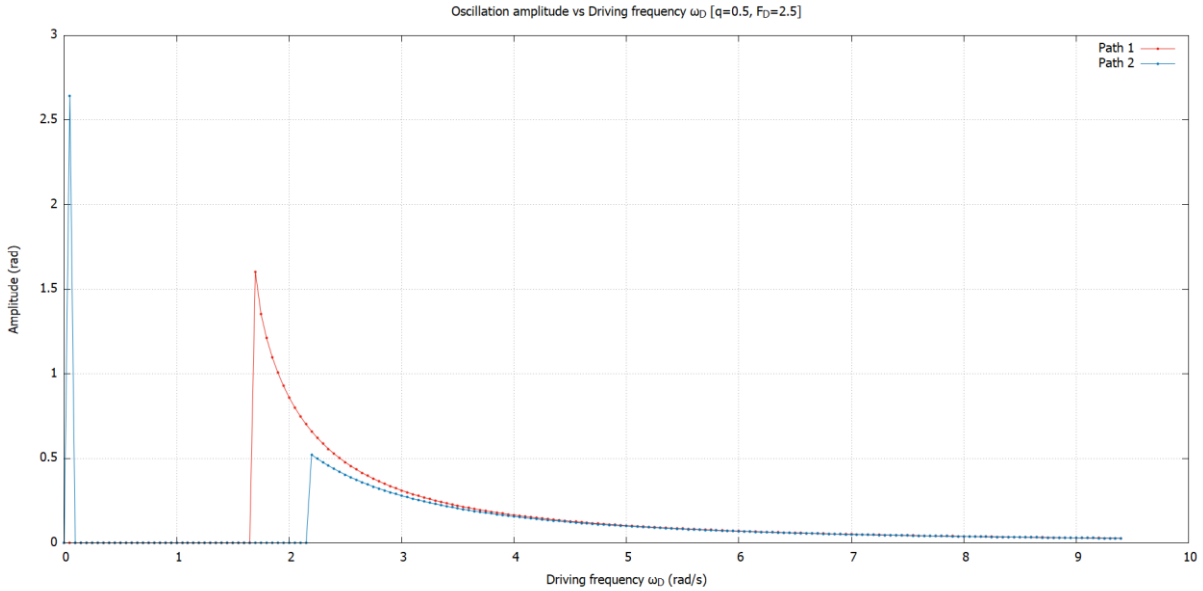

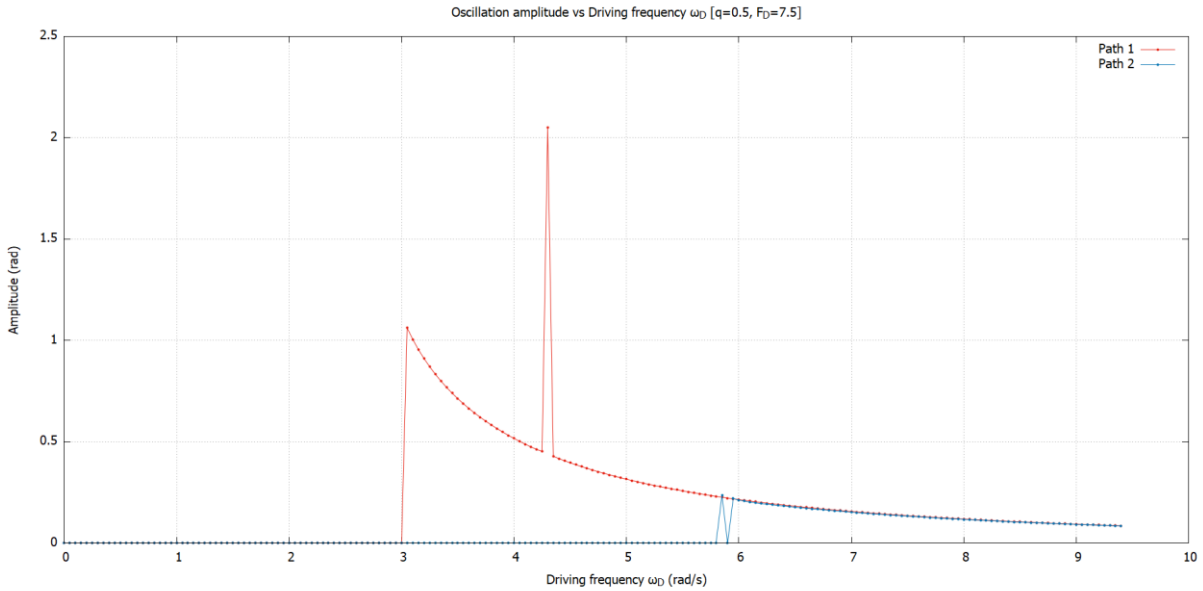

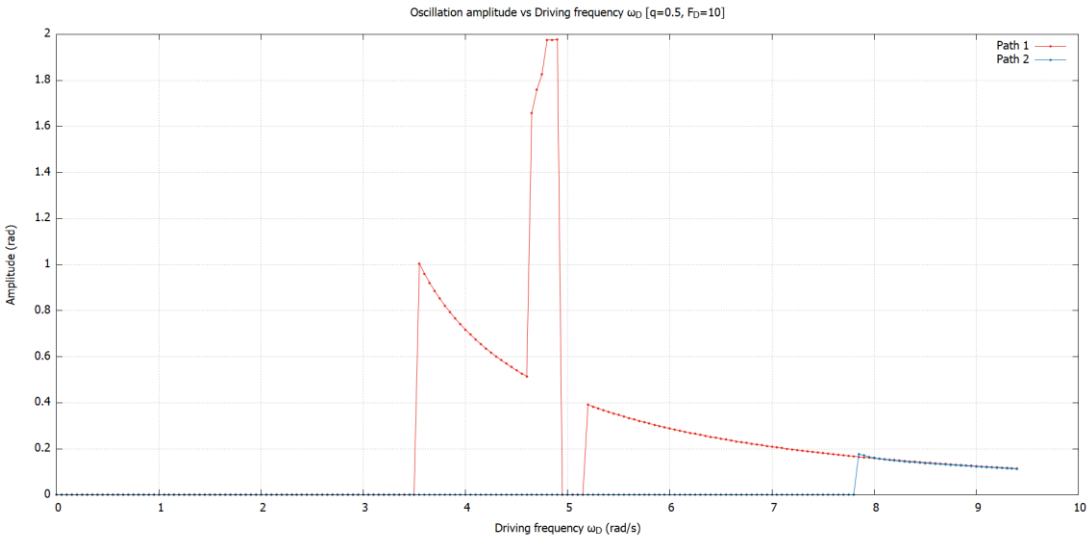

In all of the above plots, we had chosen a resolution of $d\omega_D = 0.05$ rad/s. We felt that this was small enough to capture any unusual behaviour.

Observations from the amplitude plots

Firstly, if we ignore the discontinuities, there is a clear resonant frequency ω_D that is present for both curves. But those spikes are certainly annoying. The spikes occur more frequently for C_1. These correspond, surprisingly, to "period multiplied" trajectories. While this might be an early indication of chaos, we shouldn't get our hopes too high. The "period multiplications" don't occur at the same ω_D. Ultimately, we hadn't encountered any aperiodic behaviour, which is one of the markers of chaotic motion. Moreover, chaos also entails a sensitivity to initial conditions, which we also didn't encounter.

Below, we showcase some of these anomalous "period multiplied" trajectories of $C_1 e$. Note that these trajectories are all periodic. Unlike the chaotic motion in simple pendulum, where period doubles for the same driving frequency, here period is multiplied at different ω_D.

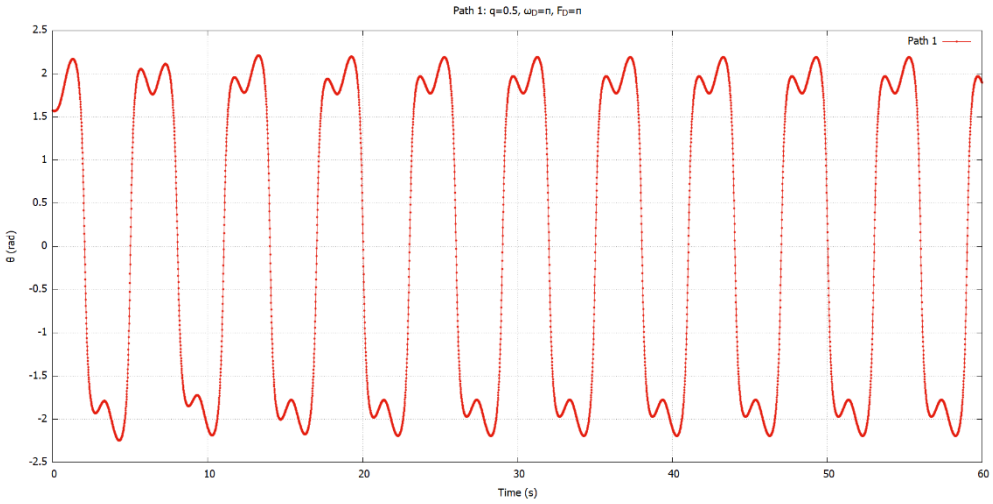

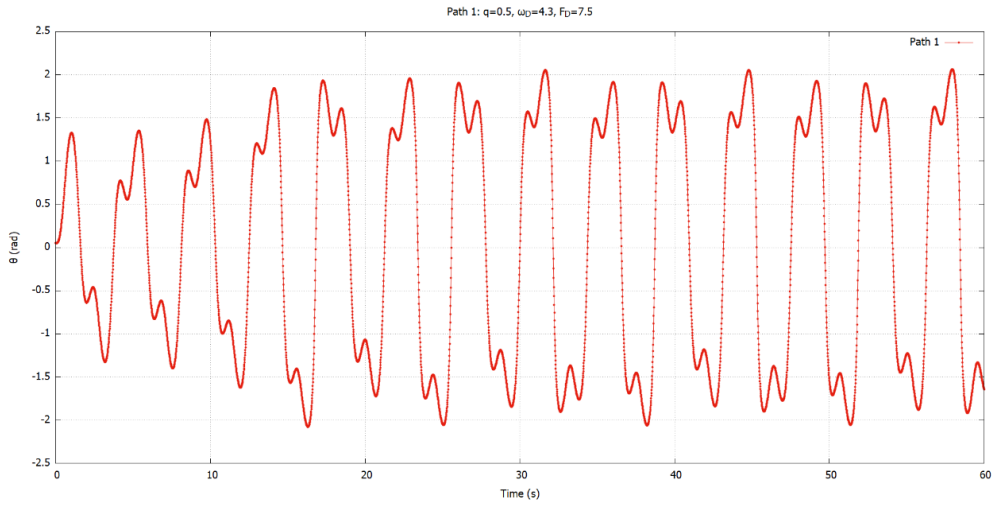

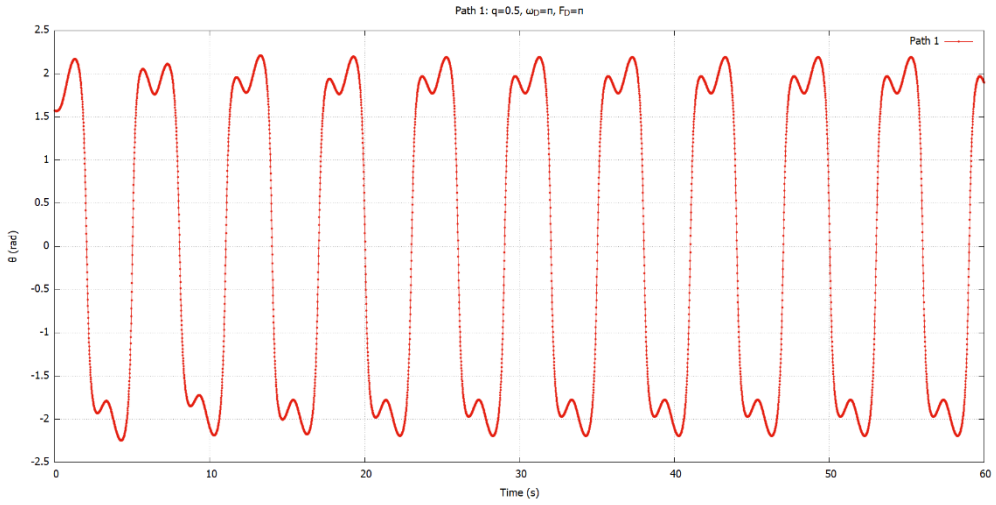

C_2, on the other hand, is quite well-behaved. The only anomaly we encountered is from the first graph from the previous page($F_D = 2.5, \omega_D = 0.05$). This is really on the verge of escaping the curve ($\theta \sim \pi$). The trajectory is shown below. Note that this too, is periodic.

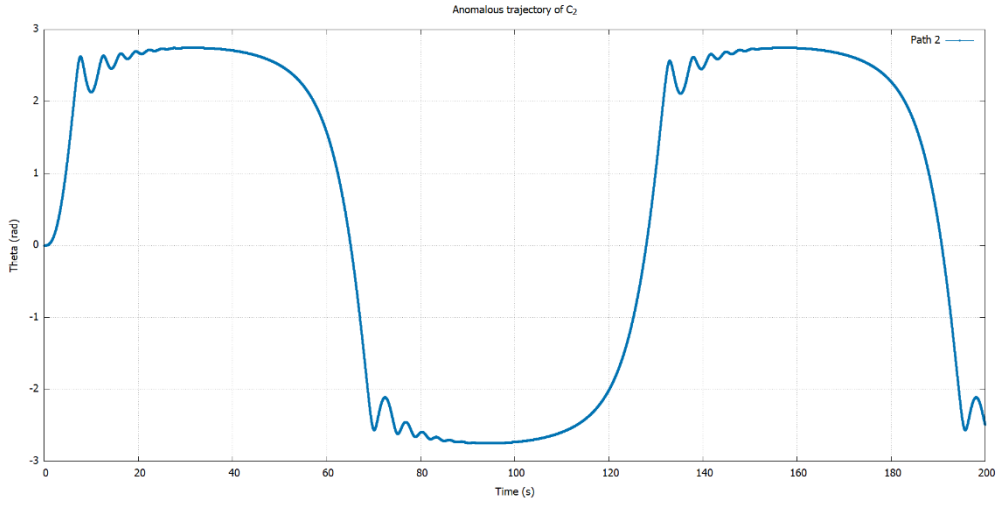

Variation of amplitude with driving amplitude F_D

For good measure, we also plotted the oscillation amplitude variation with ω_D for fixed F_D. These are the resulting plots. Again, the resolution was $dF_D = 0.05\ s^{-2}$.

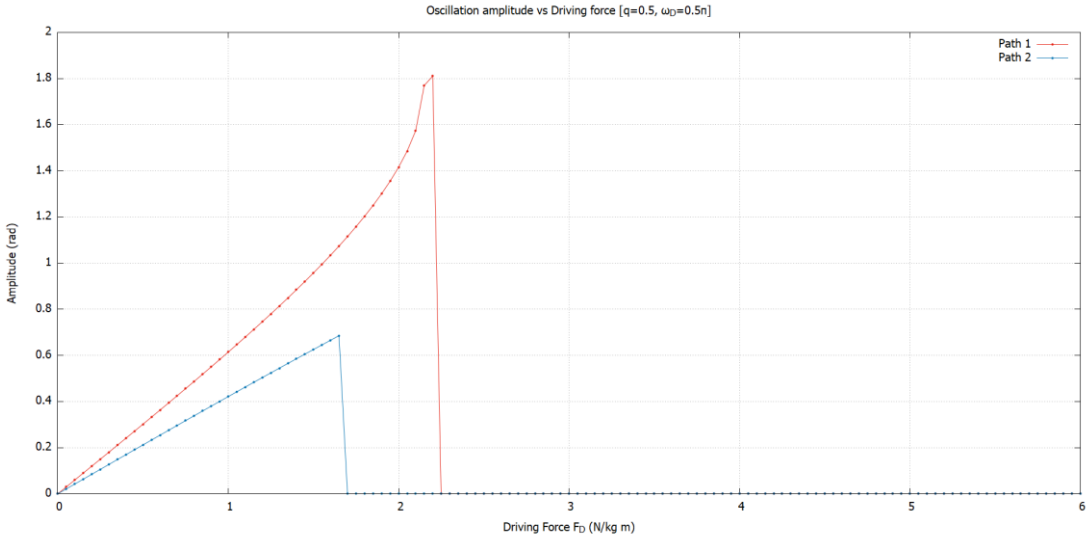

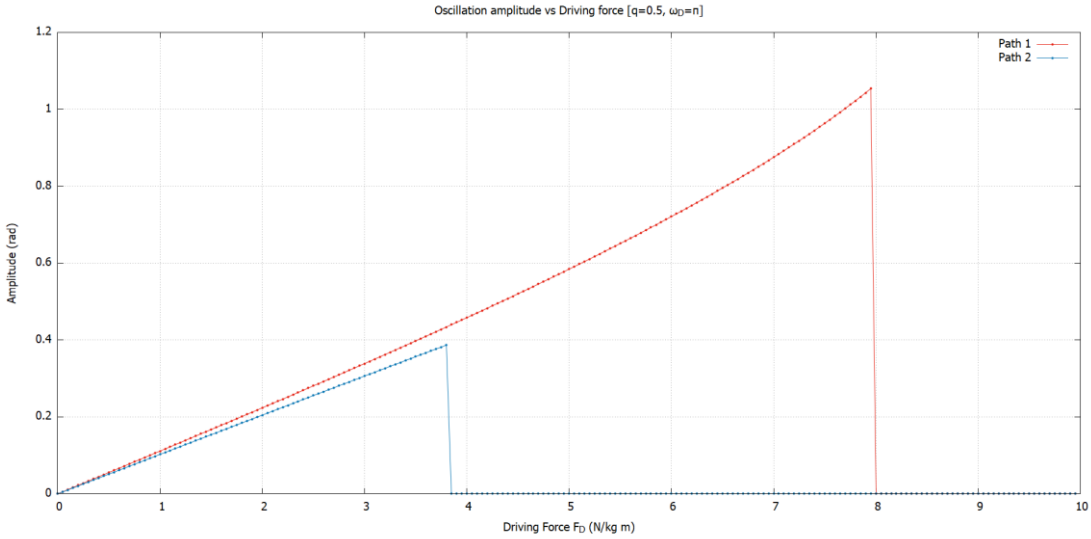

Again, no surprises here. As the driving force is increased, the system goes into overdrive, and the oscillation amplitude behaviour is somehow the reverse of the previous one. Note that the maximum amplitude is restricted for both paths. This is because there is a damping force that is present in all cases.

So, does all of the above arguments definitively rule out chaos in the given curves? Unfortunately, no. But as far as we know, these systems don't exhibit chaos, at least via the period doubling route. To completely rule out chaotic motion, we need more rigorous methods* instead of looking at a small set of parameters.

* More on this in the discussion

3.7 Conservation of Energy

We have already encountered an expression closely related to the total energy of the system in section 3.5 for C_2:

$$\text{i.e.} \quad \mathcal{L} = \frac{m\ell^2}{2}\left[1 + \cos\theta\,\dot{\theta} + \dot{\theta}^2\right] - mg\ell[1 - \cos\theta]$$

Now, $\mathcal{L} = T - V$, $E = T + V$. So, we have:

$$\mathrm{E}_2 = \frac{m\ell^2}{2}\left[1 + \cos\theta\,\dot{\theta} + \dot{\theta}^2\right] + mg\ell[1 - \cos\theta]$$

Below are 2 plots of total energy with time for C_2. Note that in all our plots, we are representing the energy for a unit mass. The first plot is un-damped:

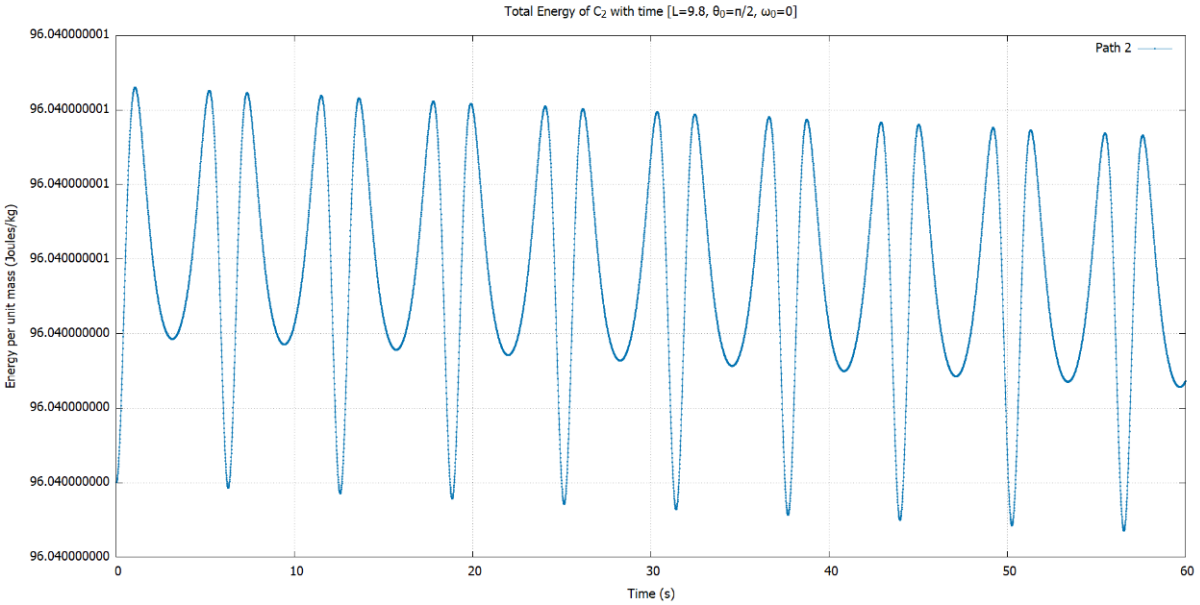

Note how little the energy variation is. The energy varies in the ninth decimal place, and it is for all practical purposes, constant.

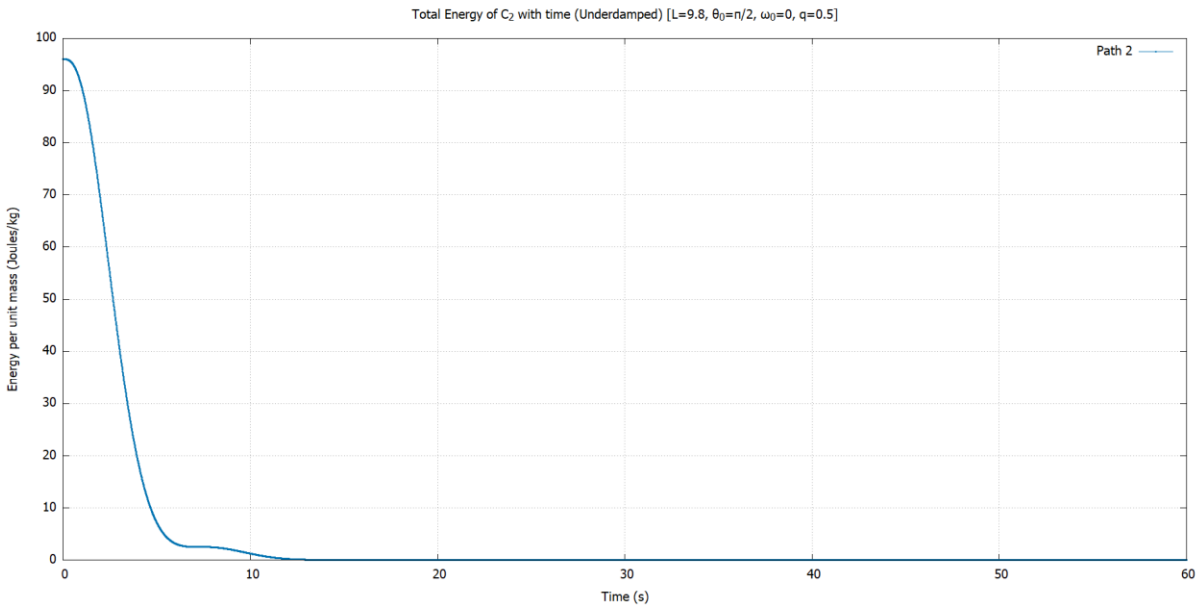

When we add a slight damping force of strength $q = 0.5$ (underdamped), we get the following plot. Note how the energy decays with time and reaches 0. This corresponds to the particle being at the equilibrium point.

Similarly, for C_1, we have:

$$\mathrm{E}_1 = T + V = \frac{1}{2}mv^2 - mgz = \frac{m}{2}[\dot{x}^2 + \dot{z}^2] + mgz$$

After some algebra later, we arrive at the following expression:

$$\frac{E_1}{m} = \frac{\ell^2\dot{\theta}^2}{(1+\cos\theta)^3} - \frac{g\ell}{(1+\cos\theta)}$$

And these are the corresponding plots:

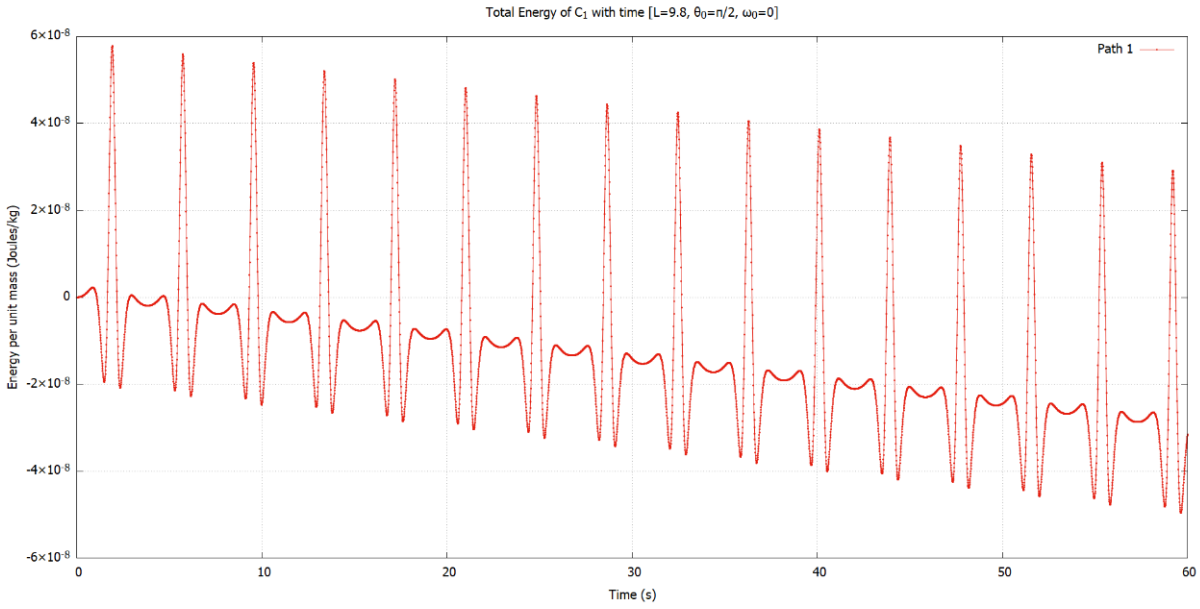

Again, the variation is extremely small, and the energy is almost constant.

When we add damping ($q = 0.5$) to the same system, we get the following plot:

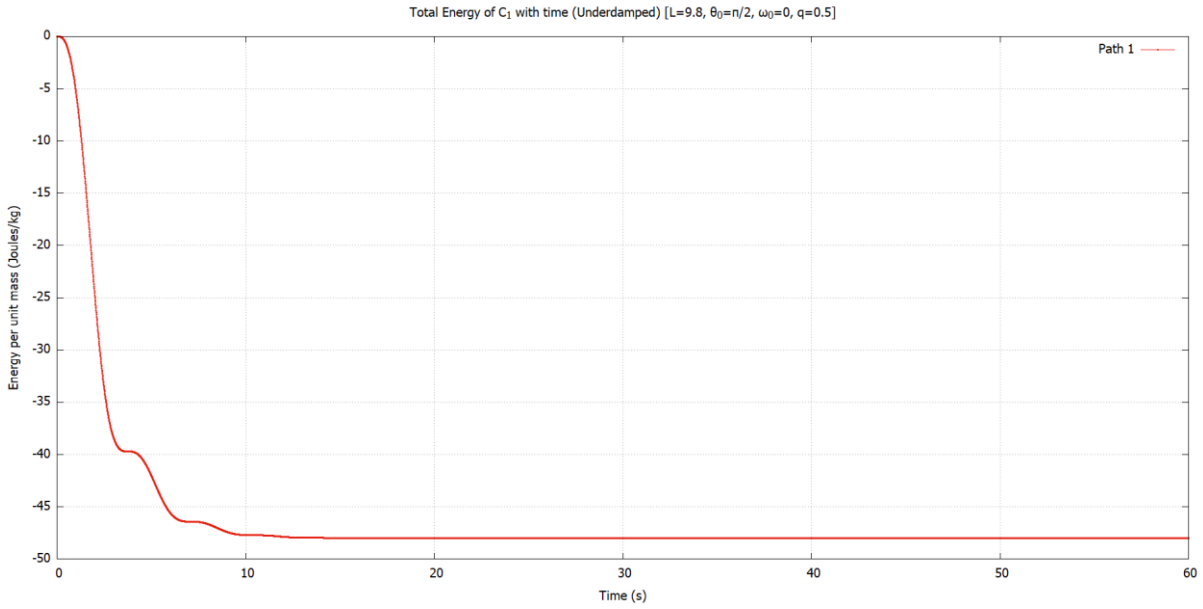

But this time, the energy doesn't settle at 0 but at some negative value. But fear not, as this is just the gravitational potential energy at the equilibrium point, which is at $(0, -\ell/2)$ for C_1.

Overall, we can say that the total energy for both curves have the expected behaviour when we simulate them with RK4 method. So, the choice of RK4 was judicious.

4 Part II: Constrained motion in 2D

4.1 Motion on the sphere

We started looking at motion on the sphere by trying out different initial conditions and looking at the corresponding phase space plots. One thing we found early on was that φ was not bound between 0 & 2π, as stated in the project document. It was actually in the range $(-\infty, \infty)$. We also found quite a few interesting behaviours that would not be physical in real life, but do occur in simulation. But first, let's have a look at some phase space plots.

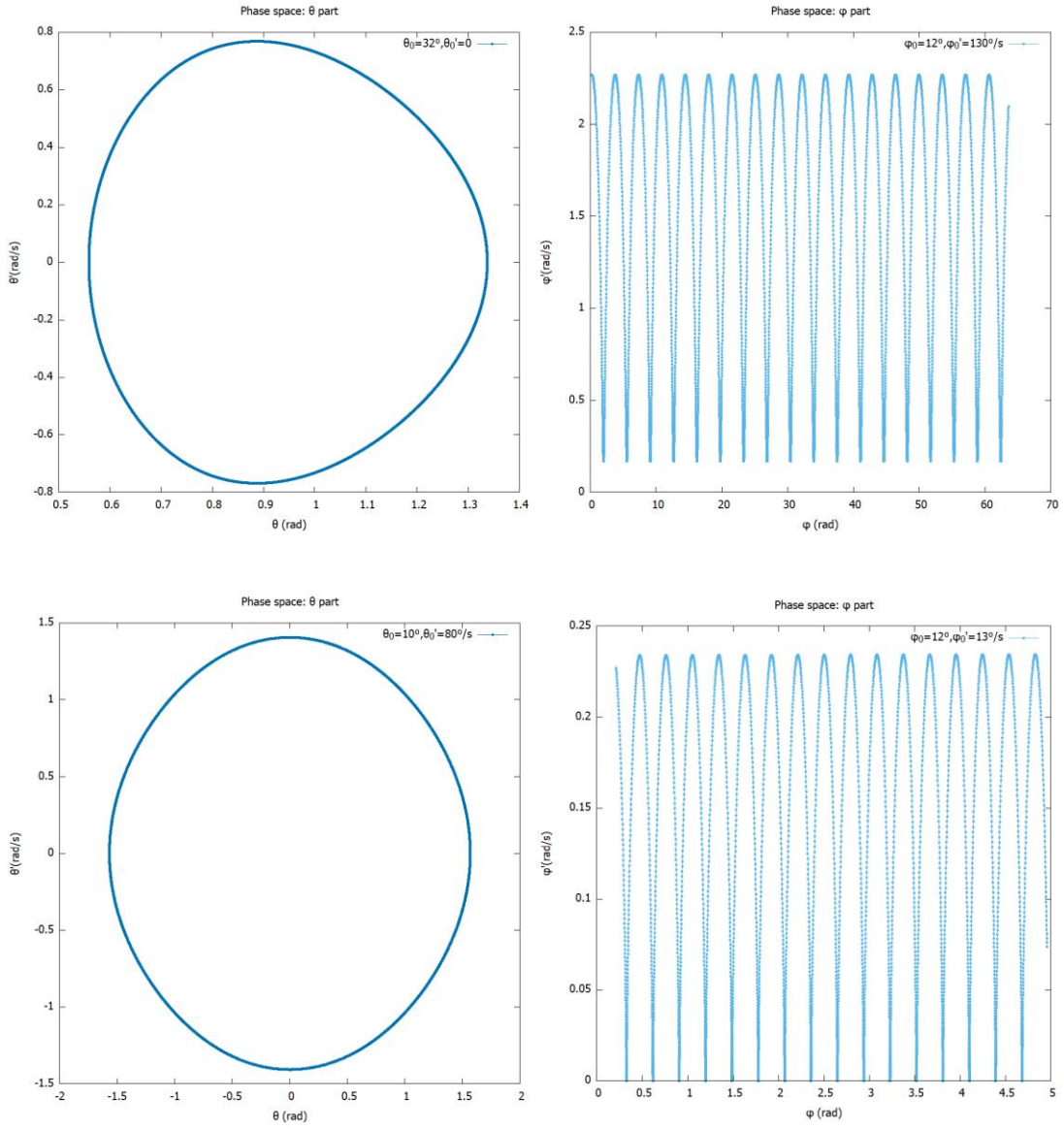

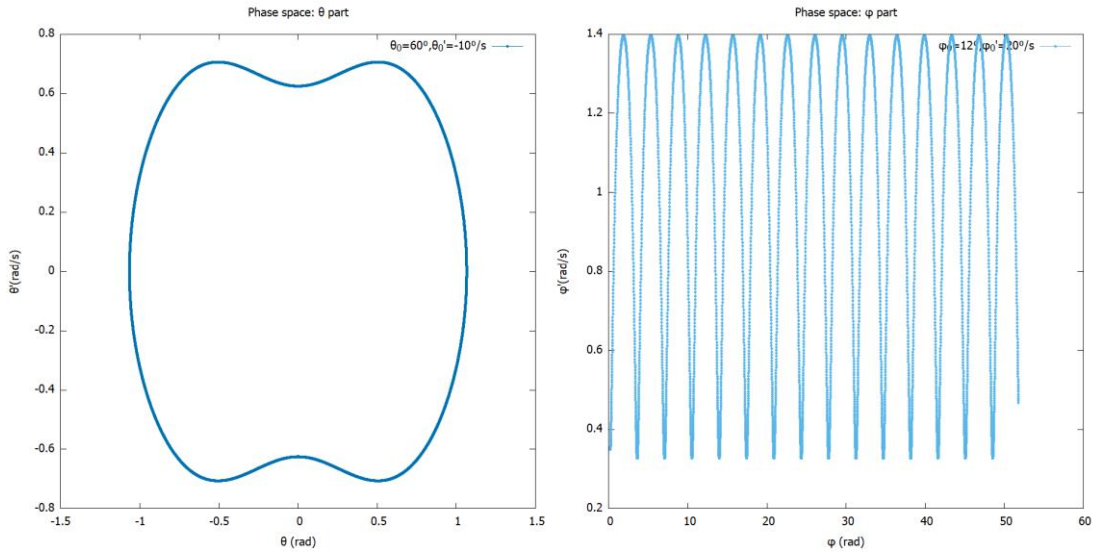

Note that this is a 3D system with a constraint. So, we have 2 degrees of freedom in total, giving us a 4D phase space. But representing a 4D figure on a 2D paper is not practical. So, we resorted to splitting the phase space into 2 branches (one for θ, another for φ). It is clear that motion along θ is oscillatory, and almost always periodic, as evidenced by the closed path in phase space. The motion in φ is more interesting. φ increases constantly, whereas the angular velocity $\dot{\varphi}$ oscillates between a certain range.

We must note that giving the system too much initial velocity results in infinities (something we encountered in C_2 in part I). But the interpretation of this is not entirely clear. We suspect that this could be an artefact of simulation or just our setup of the equations.

Now, back to the unphysical behaviour we mentioned earlier. If we place the particle at the top of the sphere ($\theta = \pi$), and setting the initial angular velocities to 0 ($\dot{\theta} = \dot{\varphi} = 0$), the particle stays put at that point. This is contrary to what would occur in real life. We would expect that the particle would drop off the top due to gravity and bounce around. This is again due to the way we set up our system.

This is also seen when we set $\theta > \frac{\pi}{2}$. Even here, we would expect the particle to fall off if no velocity is given initially. But instead, we get pendulum-like oscillations.

Maybe, interpreting these equations as motion along a spherical surface may not be accurate. A more fitting description would be to describe a mass stuck to a rigid rod of length ℓ pivoted about the origin, i.e. a "spherical pendulum".[5]

4.2 Circular path: Recreating the simple pendulum motion

As we hinted in the previous section, we can indeed recreate the motion of a simple pendulum in a spherical surface. To do so is quite simple. Just set the angular velocity along φ to be 0 ($\dot{\varphi} = 0$). The rest of the initial conditions can be freely chosen*. We can confirm that the motion is indeed along a plane by plotting the phase space.

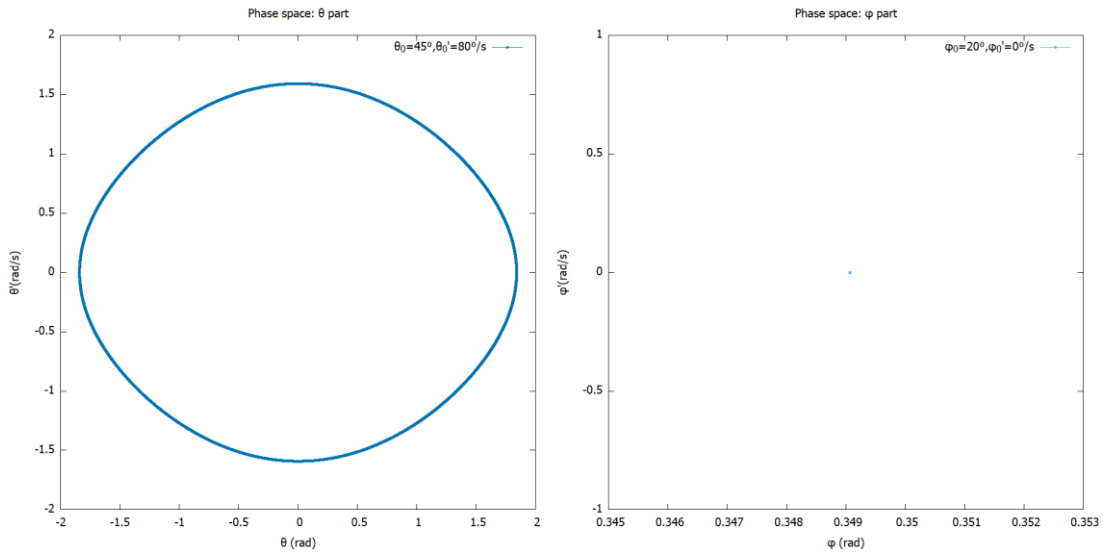

Notice that the φ branch of the phase space is just a single point, whereas the θ branch is what we typically associate with oscillatory motion. The effective degree of freedom is 1, just like the simple pendulum.

4.3 Closed paths

One of the obvious ways to achieve a closed path is simply to follow up from the previous section and increase the velocity $\dot{\theta}$ to a high enough value so that the circular path becomes closed. This is exactly what we did. But we didn't stop there. We found out that we can have closed circular path in arbitrary planes, if we adjust the velocities $(\dot{\theta_0}, \dot{\varphi_0})$ just right.

We even found closed paths that were not circular in our search for Lissajous-like figures. But the initial conditions for those are not at all trivial. Unlike Lissajous figures in the plane, where making the frequencies integer multiples of each other gave us a closed path, here it is not obvious what the condition is. In all cases, the paths we got were symmetric about φ.

How did we ascertain that the paths are indeed closed? We simulated the paths for very long times ($\sim 2000s$), and observed if the long-term path is distinct and unchanging. Paths that are not closed fill up the entire region the initial energy allows them to. So, this is a sufficient test for closed paths.

* Given the velocity is not too high

Below are some of the closed paths that we came up with, along with the initial conditions that lead to them*†. In all cases, the radius of the sphere was 9.8 m.

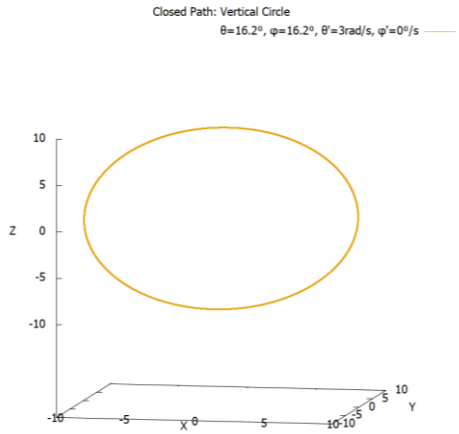

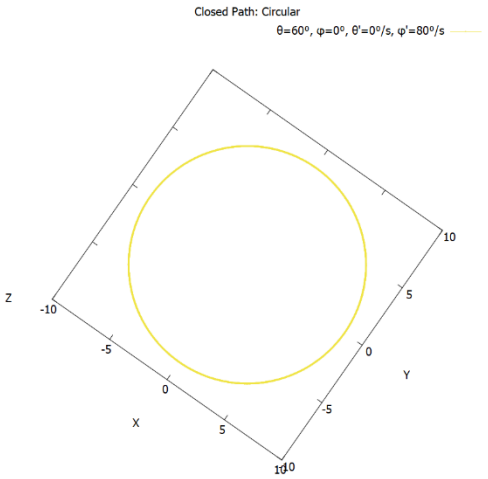

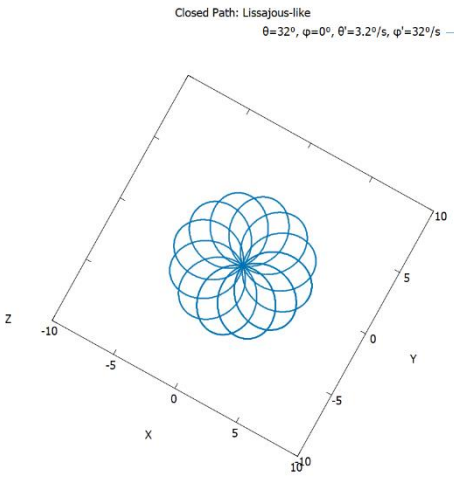

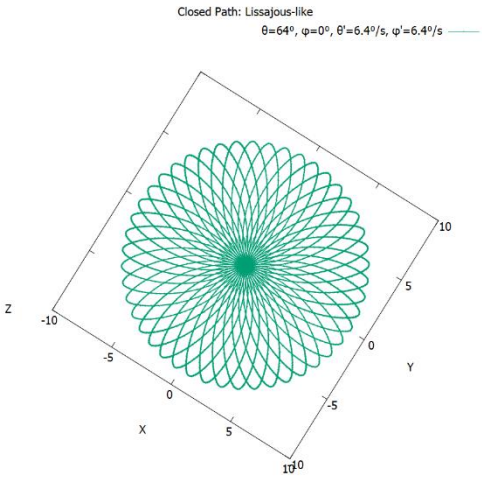

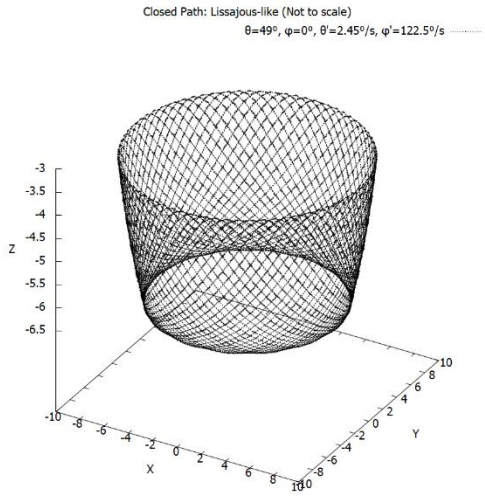

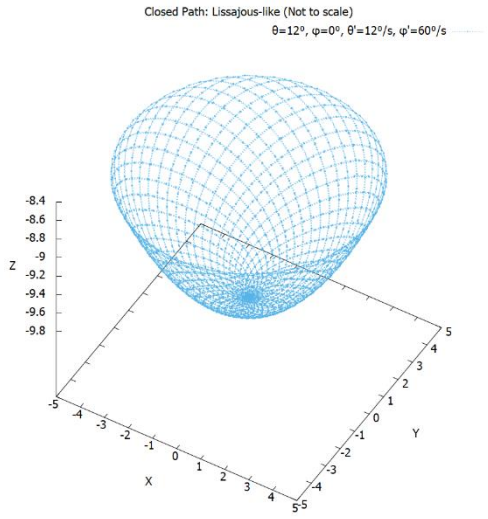

* θ' & φ' refer to the angular velocities in the figure
† Some of the figures have been rescaled for clarity

4.4 Lissajous-like figures

Firstly, what is really meant by "Lissajous-like" figures? If we are being honest, it is open to interpretations. Any given path can be considered "Lissajous-like". This is compounded by the fact that there also exists spherical Lissajous figures, that have applications in MRIs.* Whether those can be reproduced in our system is unclear.

So, to be more specific, we took inspiration from 2D Lissajous figures to come up with our very own "Lissajous-like" figures. All of them have a periodic structure about φ. And most of them are not closed (we already saw some of the closed ones). If we allow the simulation to run for prolonged durations, we see that the path covers a section of the spherical surface entirely. This behaviour is observed in the planar Lissajous figures when the ratio of frequencies is irrational. The paths below illustrate this point. We ran the simulation for the same initial condition for 60 seconds and 2000 seconds respectively.

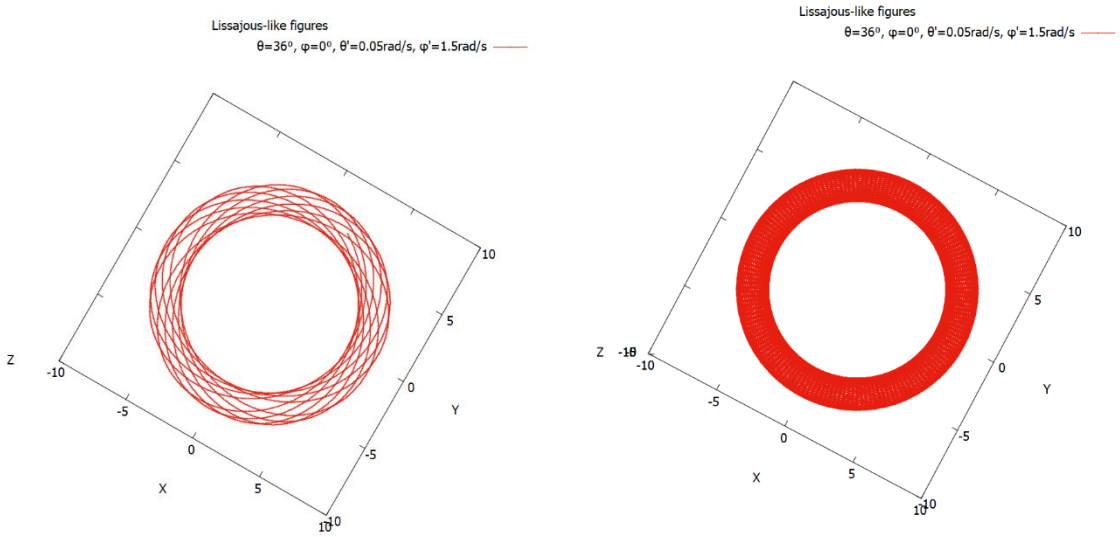

The patterns we got have quite intricate structures- some resemble flowers with numerous petals, whereas others look like baskets (like the plot above) that have a hole in the centre. But unfortunately, we cannot predict the shape just from the initial conditions.

In the following page, we showcase some of the "Lissajous-like" figures that we obtained along with the initial conditions that gave rise to them. Note that in all cases, the radius of the sphere was 9.8 m, and the simulation was run for 60 seconds.

* See: Wolfgang Erb | Spherical Lissajous Curves (unipd.it)

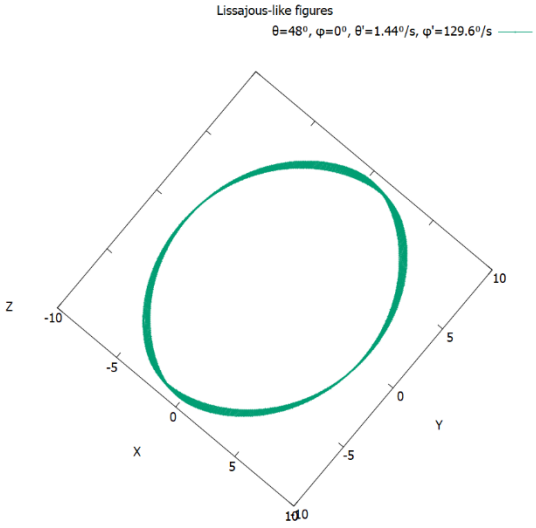
Lissajous-like figures
θ=48º, φ=0º, θ'=1.44º/s, φ'=129.6º/s
Z
X
Y

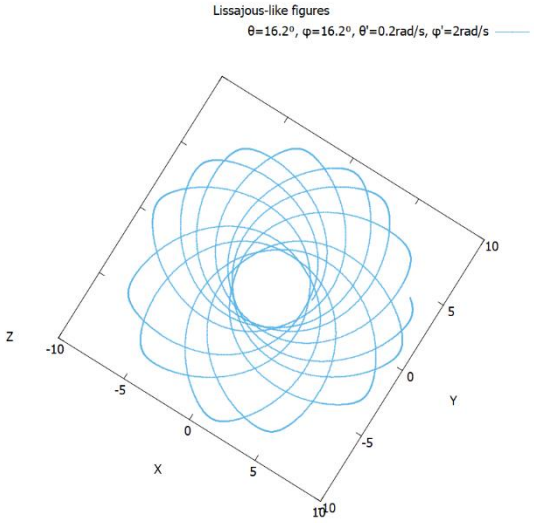
Lissajous-like figures
θ=16.2º, φ=16.2º, θ'=0.2rad/s, φ'=2rad/s
Z
X
Y

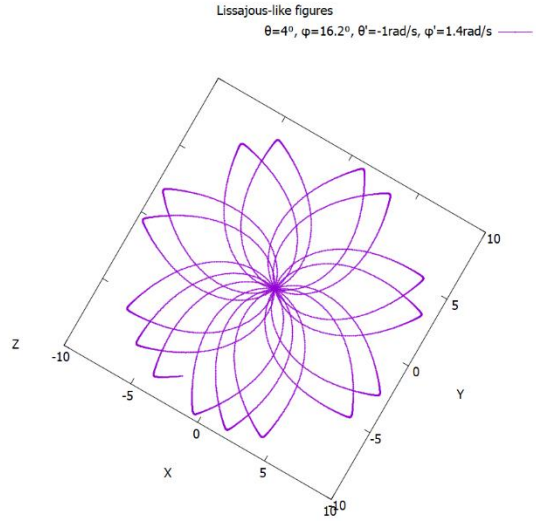
Lissajous-like figures
θ=4º, φ=16.2º, θ'=-1rad/s, φ'=1.4rad/s
Z
X
Y

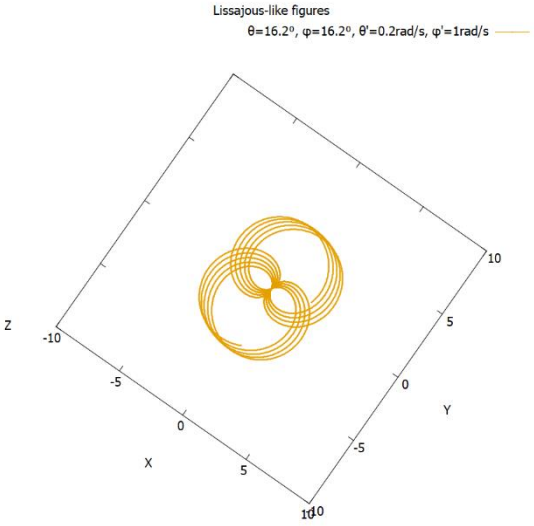
Lissajous-like figures
θ=16.2º, φ=16.2º, θ'=0.2rad/s, φ'=1rad/s
Z
X
Y

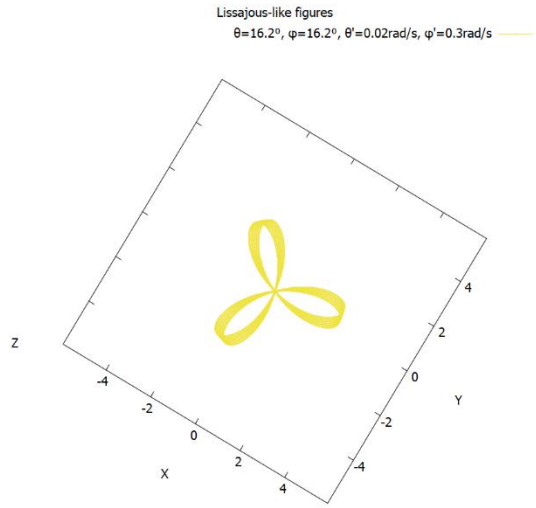
Lissajous-like figures
θ=16.2º, φ=16.2º, θ'=0.02rad/s, φ'=0.3rad/s
Z
X
Y

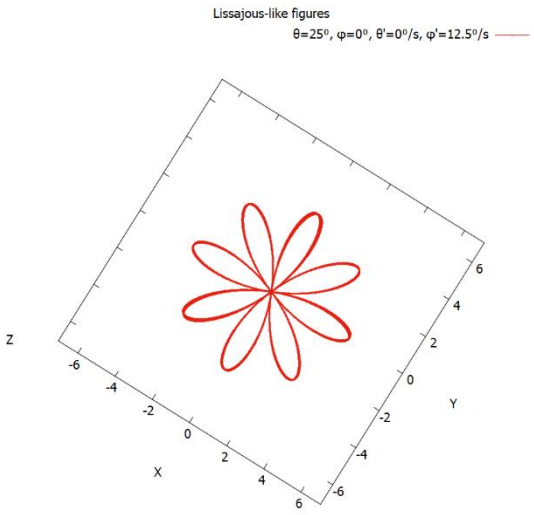
Lissajous-like figures
θ=25º, φ=0º, θ'=0º/s, φ'=12.5º/s
Z
X
Y

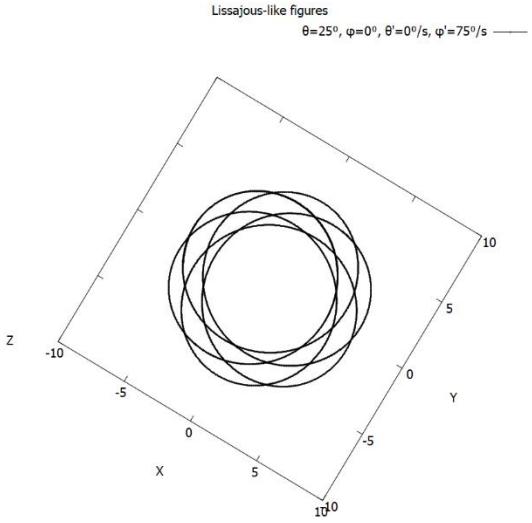

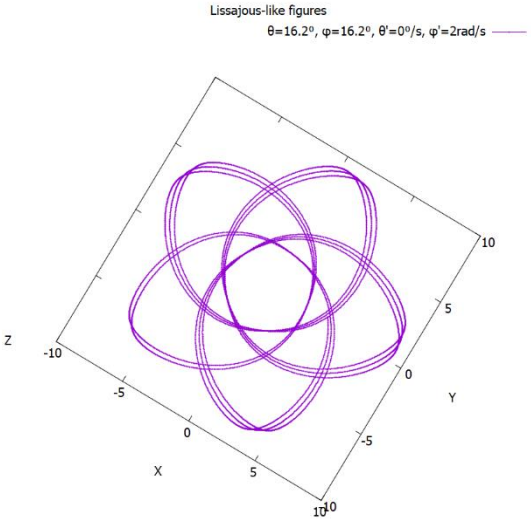

4.5 (Where is) Chaos

When looking for chaotic motion in physical systems, one of the first thing we look for is aperiodicity. That, followed by sensitivity to initial conditions are markers of a system that is chaotic. But so far, with all the initial conditions that we went through looking for closed paths and "Lissajous-like" figures, we haven't encountered either of these. Again, this does not decisively tell us that our system is not chaotic.

But we have further reasons to believe that this system isn't chaotic. For a simple pendulum, chaotic behaviour arises only when damping and driving forces are introduced. Here we have neither. By restricting our motion to the θ axis, we essentially get the simple pendulum motion back. In the absence of driving or damping forces, there is no reason to think the system is chaotic.

To be clear, we are not ruling out chaos entirely as we weren't able to investigate it rigorously. But from all the initial conditions we tried, there doesn't appear to be any markers of chaos.

4.6 Additional tasks

For this part of the project, we decided to do 2 of the given tasks: adding damping forces and the motion on a hemispherical surface.

(b) Adding damping forces

We have several possibilities when considering a damping force. But the one we found most natural was to imagine the sphere to be filled with a viscous fluid of different concentrations. This means that the damping force is isotropic and homogeneous. Also, we assume that the damping force varies linearly, and opposite to the angular velocities. The equations of motion then become:

$$\ddot{\theta} = \dot{\varphi}^2 \sin\theta \cos\theta - \frac{g}{\ell}\cos\theta - q\dot{\theta}$$

$$\ddot{\varphi} = -\frac{2\dot{\theta}\dot{\varphi}\cos\theta}{\sin\theta} - q\dot{\varphi}$$

Here, q has units of s^{-1}. The resulting motion exhibits the usual behaviour, i.e. we get both underdamped and overdamped motion. This implies the existence of critical damping, but we haven't found the corresponding damping coefficient.

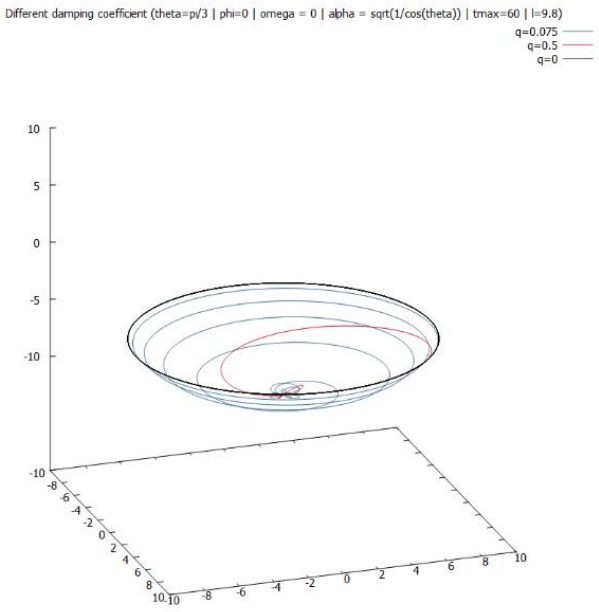

The figure above illustrates the effect of damping*. We plotted the paths for the same initial condition, but with 3 different damping coefficients q. In the presence of damping, the particle gradually loses its energy and settles at the bottom of the sphere. This is in fact the stable equilibrium point of the hemisphere.

* Here `theta` & `phi` are in rad. `alpha` ($\dot{\varphi}$) & `omega` ($\dot{\theta}$) are in rad/s

(d) Realistic motion on a hemispherical surface

We've encountered an anomaly in section 4.1. When we release a particle from the upper hemisphere, instead of falling vertically down, it sticks to the sphere as if it was on the outside. This means that the spherical surface may not be the best interpretation of this system. To make the motion more realistic, we considered the motion on a hemisphere instead. We chop off the upper hemisphere, leaving us with: $0 \leq \theta < \frac{\pi}{2}$

We've already seen how the motion on the sphere looks like. For low initial angular velocities, the motion is the same here. For higher angular velocities, the particle escapes the hemispherical bowl. In general, we predict that the particle will continue like a projectile under gravity (i.e. a parabolic trajectory).

While we set out to study the motion in the most general case, we couldn't complete the relevant code in time. We did manage to simulate a special case: when the azimuthal angular velocity is 0 ($\dot{\varphi}$=0). For this case, we essentially have one degree of freedom. The velocity as the particle escapes the bowl is directly upwards (i.e. $\vec{v} = v_z\hat{z}$).

The projectile motion is triggered if the displacement along z is positive. We simulated the projectile using Euler method*. In the resulting motion, the particle is seen to escape the bowl, continue straight up, and fall down and continue motion in the bowl and escape at the other end. We have created a fountain. We even added a damping force† and found that the particle dissipates energy and settles down at the bottom. Below are some of the trajectories.

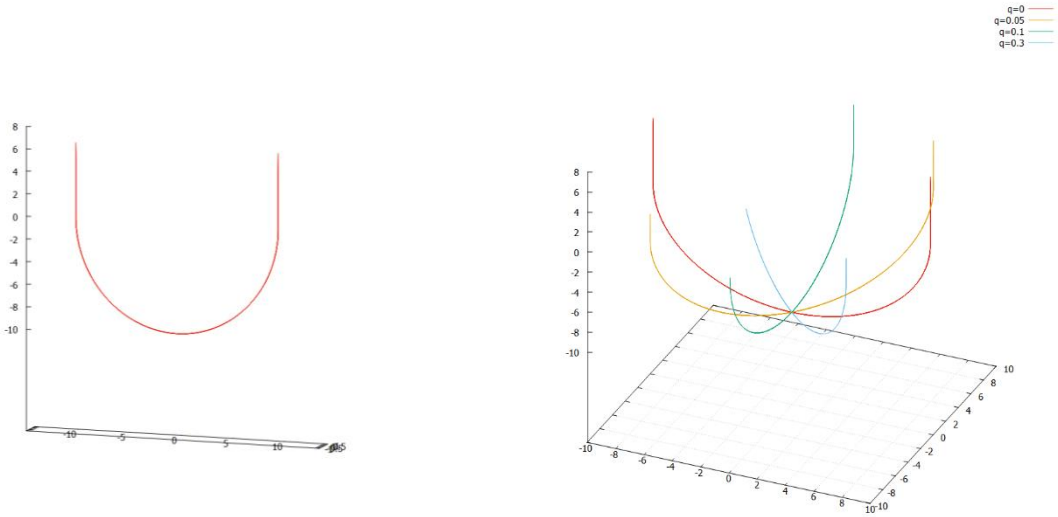

* Which we note is a bad choice, as it has a bad reputation for energy conservation
† The one we discussed previously

4.7 Conservation of energy & angular momentum*

As we suggested before, our system is actually better interpreted as a spherical pendulum. In fact, we can use the energy equation of the spherical pendulum for our system. The relevant equation is:

$$\frac{E}{m} = \frac{1}{2}\ell^2[\dot{\theta}^2 + \sin^2\theta\,\dot{\varphi}^2] - g\ell\cos\theta$$

As for angular momentum, we found out from different sources that only the angular momentum about z axis is conserved. The angular momenta about x & y axes are not conserved [6]. The equation for reduced angular momentum about z axis is as follows:

$$\frac{L_z}{m} = \ell^2[\dot{\theta}^2 + \sin^2\theta\,\dot{\varphi}^2]$$

Here are the results we obtained for different scenarios:

- **Simple pendulum:**

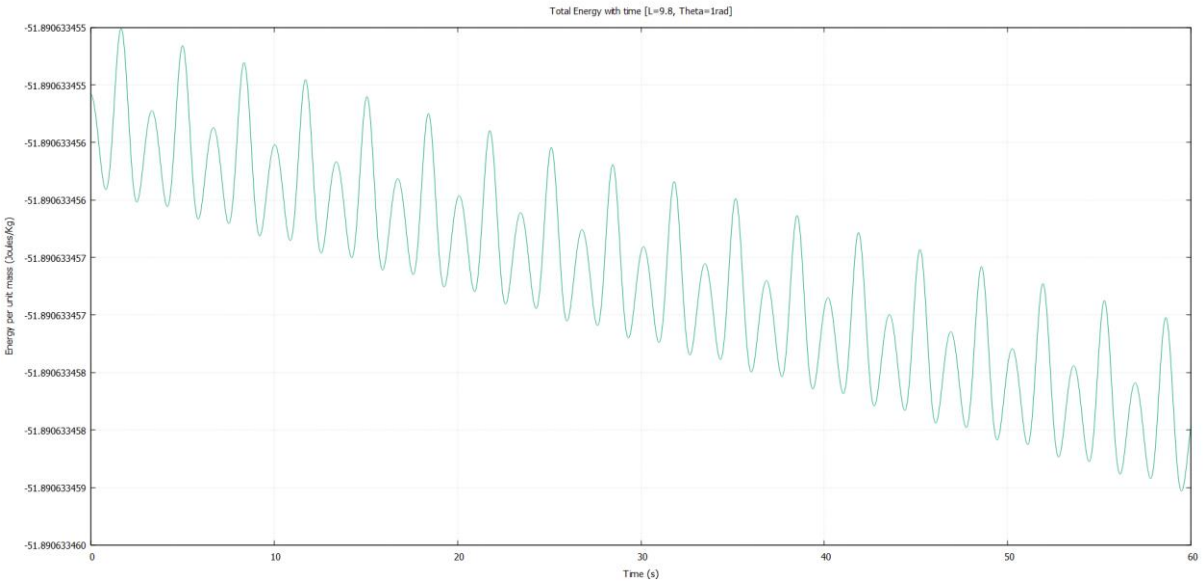

For initial conditions that recreate the simple pendulum motion, the variation in total energy resembles the ones we encountered in part I. There is a miniscule decrease with time, but that is negligible for practical purposes. So energy is conserved here.

As for the angular momentum in z axis, it stays constant at 0 throughout the motion. So that is conserved as well.

* The graphs of angular momenta should read angular momentum in Z-axis. We noticed it too late.

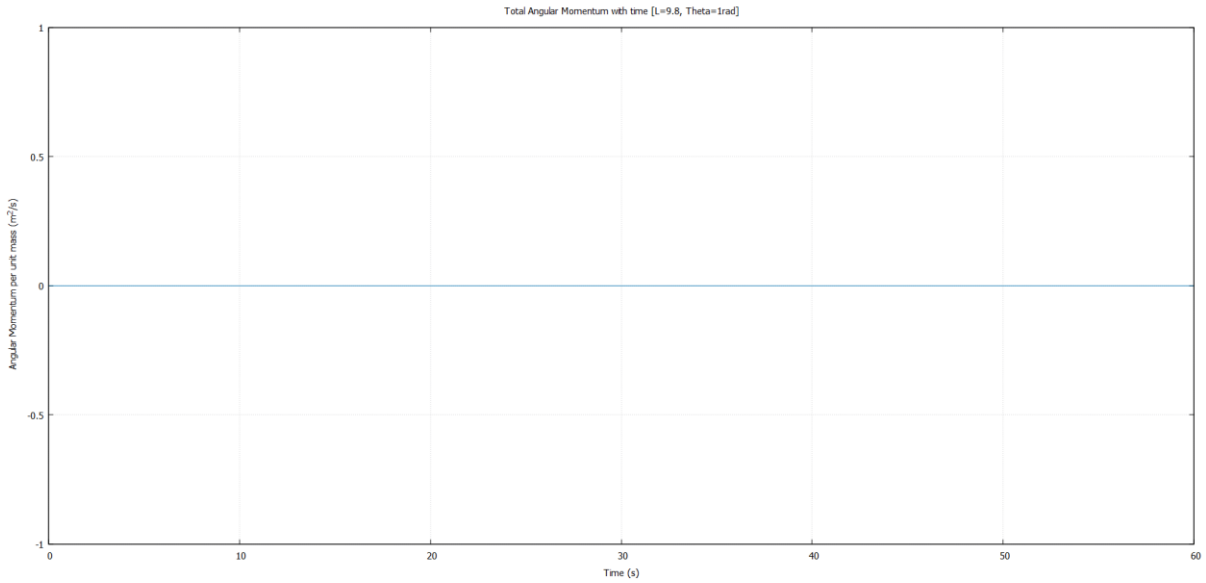

- **Circular path**

For initial conditions corresponding to a circular path, the total energy is again conserved. The variations that occur may be attributed to machine precision error.

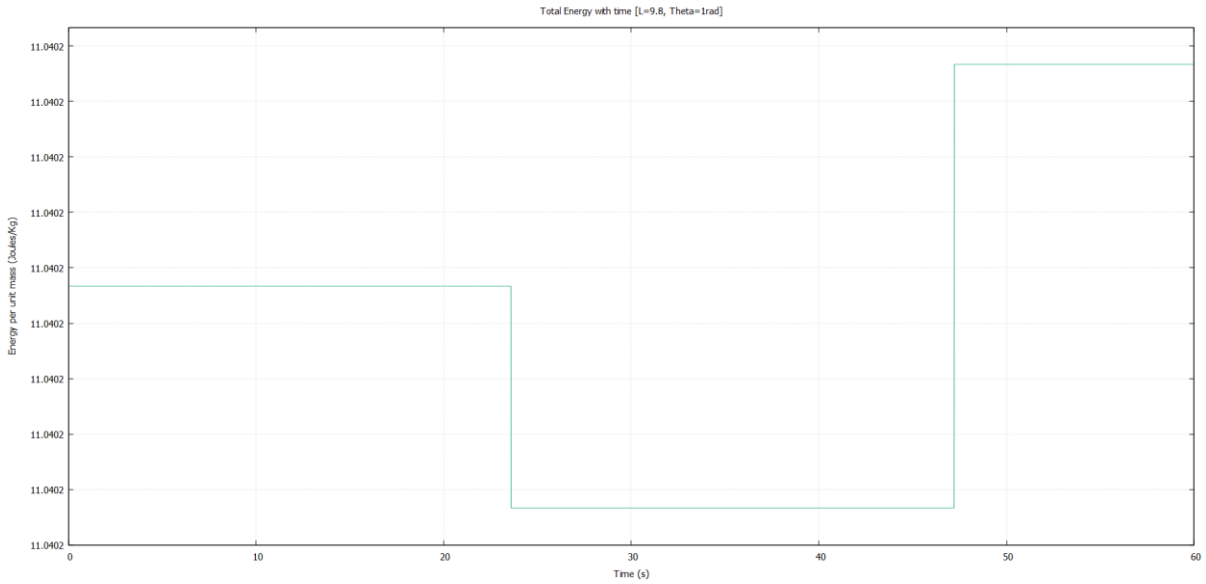

The angular momentum has a similar graph, and it too is conserved.

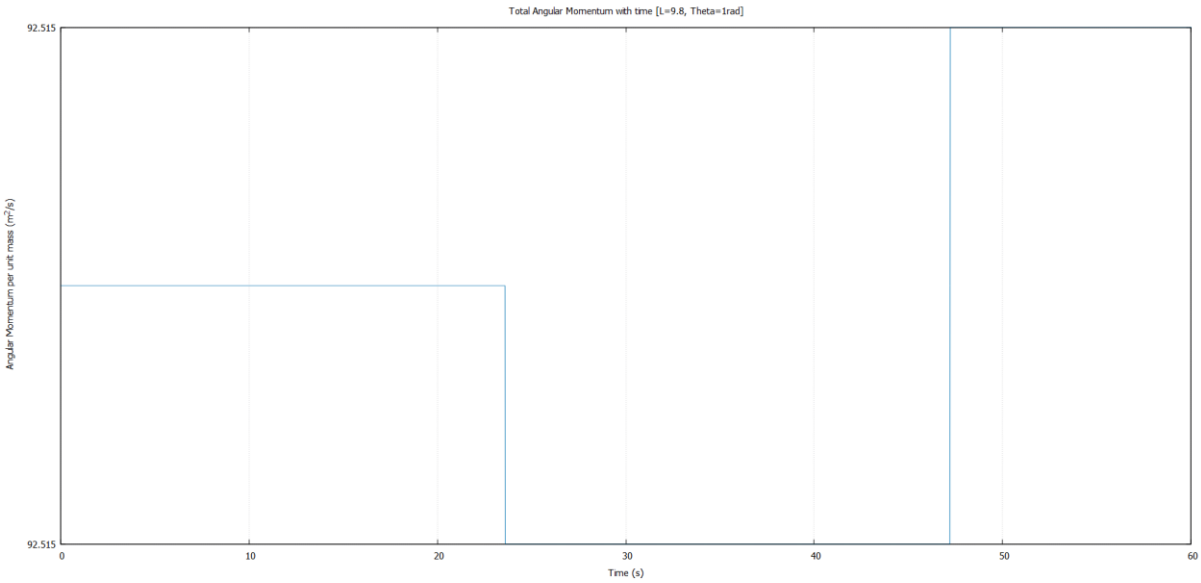

- **Arbitrary paths**

To our surprise, the total energy and angular momentum in *z* axis is not conserved for arbitrary paths with 2 degrees of freedom. Both oscillate wildly with time. While we can argue that the average remains almost constant, this is not the expected behaviour from a physical system.

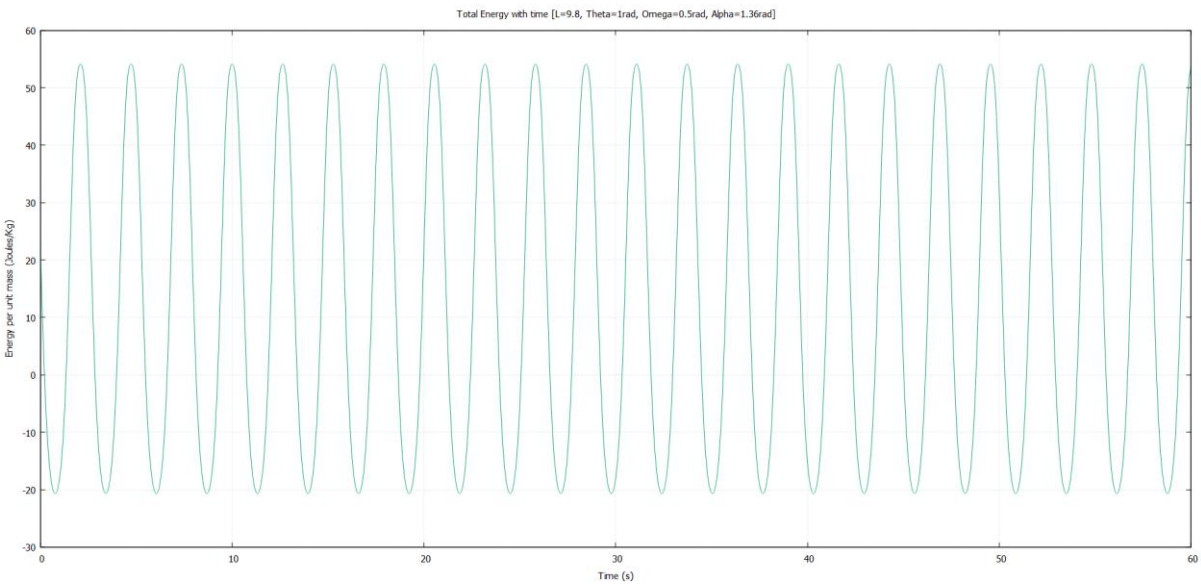

If we plot the kinetic and potential energies separately, we find that they oscillate at almost the same frequency and phase, but their amplitudes have a mismatch. Perhaps this might explain the unusual oscillations.

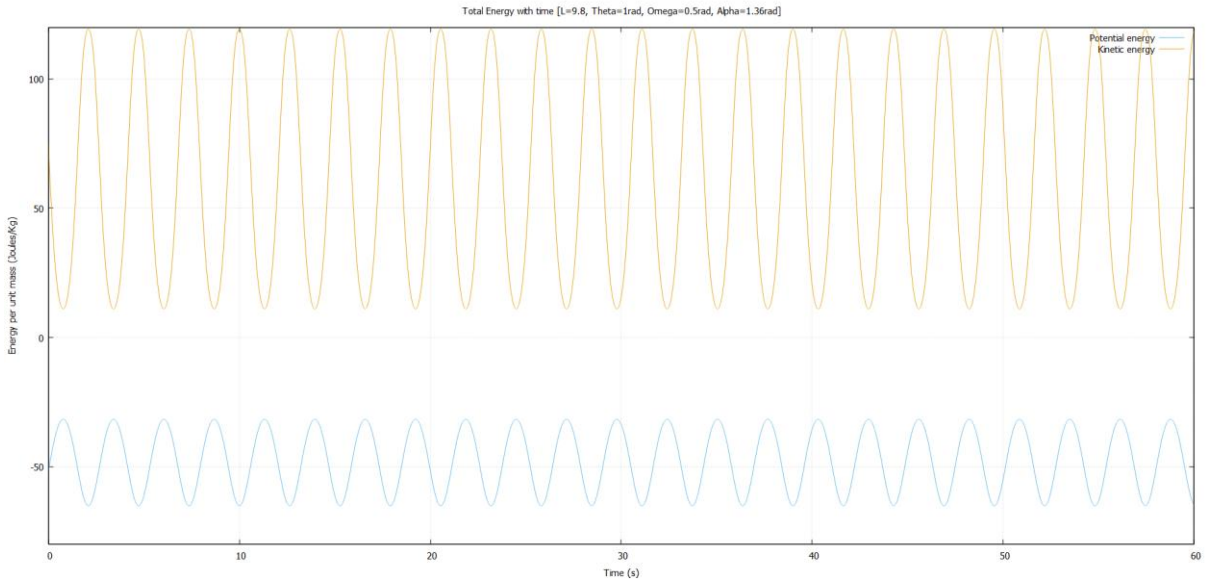

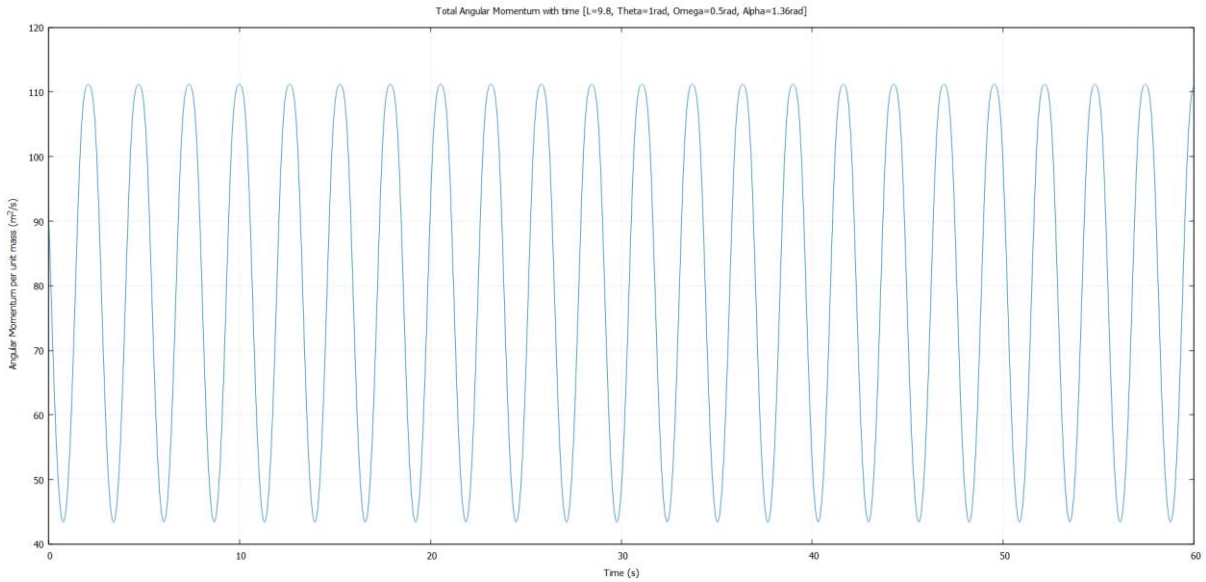

The story is the same for angular momentum. So in general, we cannot conclude that energy and z component of angular momentum is conserved. And painfully, we don't have a good explanation for these anomalies. Our analysis here remains incomplete. This section needs to be revisited in future.

5 Discussion

5.1 Part I

Measuring period

One of the first hurdles we faced was reliably measuring the period directly from the code. We tried doing this by finding the time at which the system returns to its initial angular velocity. But the results were less than good.

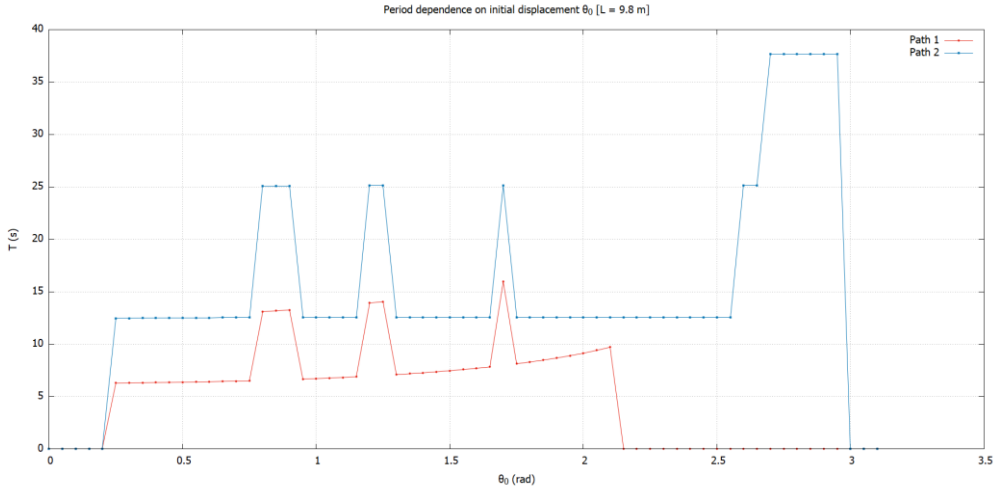

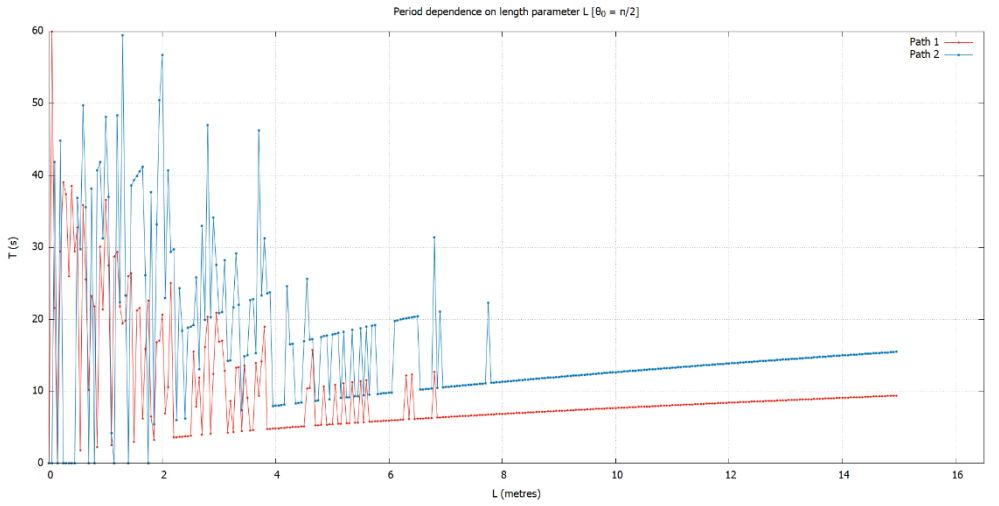

But luckily, we figured out that varying the tolerance in our code gave good results in different ranges of θ_0 & ℓ. Stitching together the data from several of these runs fixed this issue for the most part. We only had to fix a handful of data points manually or from the simulation directly.

A much better way to measure period would be to use a discrete time Fourier transform of our trajectory and look at the spikes in frequency space.[7]

Fitting the period data

One of the things that we tried to do and partially succeeded was coming up with a general expression of period for both curves C_1 & C_2 for any given length ℓ and oscillation amplitude θ_0. Our expression for C_1 was not very accurate. This was because our analysis of length dependence was not complete. We only looked at the ℓ dependence for $\theta_0 = \pi/2$. And even then, we could only conclude that the dependence was to its square root. More analysis is required here to get a more accurate expression. We should also attempt deriving the periods analytically.

Investigation of chaos

With addition of damping and driving forces to the curves, we might've expected to see some chaotic behaviour like we did with the simple pendulum. Instead, all the trajectories we encountered were periodic. For C_1, we actually found period multiplied paths. But we only looked into a small space of the driving parameters. And we haven't tried decreasing the time-step from $dt = 0.01s$.

Also, we didn't test the sensitivity to initial conditions rigorously. We can do this by calculating the Lyapunov exponents of the systems.

Comparison with simple pendulum

One of the things that we ought to do in the future is to compare our results with a well-known system, like the simple pendulum. That way, we can put our results into perspective and make predictions about similar systems.

More damping forces

In our project, we've dealt exclusively with linear damping forces, i.e. $F \propto \dot{\theta}$. It would be interesting to see the effects of non-linear damping forces of the form $F \propto \dot{\theta}^n$ and see if we still get the same behaviour, including chaos (or lack of it).

Infinities in driven motion

We found that the trajectories blow up for large driving amplitudes and low driving frequencies, which is not accounted for completely (for C_1). Here again, we haven't tried changing the time-step. This might also give us a different result for chaotic motion.

5.2 Part II

Closed paths

In this project, we only came up with closed paths that were either circular or on a hemisphere. We haven't considered paths that went around the full sphere. It would be interesting to see if such paths even exist. We also note that due to azimuthal symmetry, the initial φ position doesn't matter.

"Lissajous-like" figures

For "Lissajous-like" figures, we focused entirely on the 2D path on the sphere itself. We didn't look into the figures when projected into different planes. This might produce figures that are more fitting of this title.

Investigation of chaos

A lot of what we said about chaos in part I applies here. But here, we are quite certain that chaotic motion is not likely. Most literature that discuss chaos have damping and driving forces.[8] But again, we would like to calculate the Lyapunov exponents to confirm this.

Conservation of energy & angular momentum

We saw that the total energy is not conserved in general. The energy-time graph had large oscillations. One reason for this might be that our energy expression was not correct. Another might be that our implementation in the code was faulty. But that doesn't completely explain why the energy is conserved when motion is restricted to a plane.

Due to brevity of time we couldn't derive the angular momentum expressions properly. This is something that we have to revisit to complete our analysis.

Optional tasks

As we mentioned, our optional task is not completed. Our ultimate goal is to be able to simulate the trajectory of a particle with any given initial condition. We could also investigate the range of motion for different initial conditions and the conditions for maximum range. This, in addition to implementing spherical collisions would make for a very interesting system.

6 Conclusion

Over the course of this project, we studied constrained motion along different surfaces. In part I, we studied the motion on a parabola and a cycloid. We investigated the properties of periodic motion, which allowed us to identify the cycloid. We tried to derive a general expression for the period by studying the dependence of period on various parameters. Adding damping forces to the motion yielded the expected behaviour, but driving forces led to some unusual infinities.

In part II, we investigated motion on a sphere, and found that the system is better interpreted as a spherical pendulum. We came up with initial conditions that recreated the motion of a simple pendulum, closed paths and "Lissajous-like" figures.

Our investigation of chaos led us to a dead end in both parts. While we expect that the spherical pendulum is not chaotic in the absence of damping and driving forces, our analysis wasn't rigorous. We did find some period multiplied trajectories on the parabola, but no aperiodicity.

We found that energy conservation holds quite well in part I. In part II, energy and angular momentum were conserved only for motion in a plane. Our analysis for angular momentum was incomplete.

At the end, constrained motion is quite rich and surprising in the most unexpected of ways. It was a pleasure studying it and doing this project.

References

[1] Runge–Kutta methods. (2021, November 17). Retrieved January 13, 2022, from https://en.wikipedia.org/wiki/Runge–Kutta_methods#Explicit_Runge–Kutta_methods

[2] Holonomic constraints. (2021, September 26). Retrieved January 13, 2022, from https://en.wikipedia.org/wiki/Holonomic_constraints

[3] Routes to chaos. Retrieved January 13, 2022, from https://encyclopediaofmath.org/wiki/Routes_to_chaos#References

[4] Sandri, M. (1996). Numerical calculation of Lyapunov exponents. *Mathematica Journal*, *6*(3), 78-84.

[5] Spherical pendulum. (2021, December 17). Retrieved January 13, 2022, from https://en.wikipedia.org/wiki/Spherical_pendulum

[6] (https://physics.stackexchange.com/users/196140/eli), Eli. *Spherical pendulum torque and angular momentum*. Physics Stack Exchange https://physics.stackexchange.com/q/604114

[7] (https://math.stackexchange.com/users/53268/ron-gordon), Ron Gordon. *How to find the period of a periodic function?* Math Stack Exchange https://math.stackexchange.com/q/307984

[8] Bryant, P. J. (1993). Breakdown to chaotic motion of a forced, damped, spherical pendulum. *Physica D: Nonlinear Phenomena*, *64*(1-3), 324-339.